

מכון ויצמן למדע

WEIZMANN INSTITUTE OF SCIENCE



## Assembly of Synthetic Functional Cellulosomal Structures onto the Cell Surface of *Lactobacillus plantarum*, a Potent Member of the Gut Microbiome

### Document Version:

Accepted author manuscript (peer-reviewed)

### Citation for published version:

Stern, J, Morais, S, Ben-David, Y, Salama, R, Shamshoum, M, Lamed, R, Shoham, Y, Bayer, EA & Mizrahi, I 2018, 'Assembly of Synthetic Functional Cellulosomal Structures onto the Cell Surface of *Lactobacillus plantarum*, a Potent Member of the Gut Microbiome', *Applied and Environmental Microbiology*, vol. 84, no. 8, e00282-18. <https://doi.org/10.1128/AEM.00282-18>

Total number of authors:

9

### Digital Object Identifier (DOI):

[10.1128/AEM.00282-18](https://doi.org/10.1128/AEM.00282-18)

### Published In:

Applied and Environmental Microbiology

### License:

Unspecified

### General rights

@ 2020 This manuscript version is made available under the above license via The Weizmann Institute of Science Open Access Collection is retained by the author(s) and / or other copyright owners and it is a condition of accessing these publications that users recognize and abide by the legal requirements associated with these rights.

### How does open access to this work benefit you?

Let us know @ [library@weizmann.ac.il](mailto:library@weizmann.ac.il)

### Take down policy

The Weizmann Institute of Science has made every reasonable effort to ensure that Weizmann Institute of Science content complies with copyright restrictions. If you believe that the public display of this file breaches copyright please contact [library@weizmann.ac.il](mailto:library@weizmann.ac.il) providing details, and we will remove access to the work immediately and investigate your claim.

1 **Assembly of synthetic functional cellulosomal structures onto**  
2 **the *Lactobacillus plantarum* cell surface – a potent member of**  
3 **the gut microbiome**

4

5

6 Johanna Stern<sup>a\*</sup>, Sarah Morais<sup>a, b\*</sup>, Yonit Ben-David<sup>a</sup>, Rachel Salama<sup>c</sup>, Melina  
7 Shamshoum<sup>a</sup>, Raphael Lamed<sup>d</sup>, Yuval Shoham<sup>c</sup>, Edward A Bayer<sup>a</sup> and Itzhak Mizrahi<sup>b†</sup>

8

9 *<sup>a</sup>Department of Biomolecular Sciences, The Weizmann Institute of Science, Rehovot 7610001*  
10 *Israel;*

11 *<sup>b</sup>Faculty of Natural Sciences, Ben-Gurion University of the Negev, Beer-Sheva 8499000 Israel*

12 *<sup>c</sup>Department of Biotechnology and Food Engineering The Technion Israel Institute of*  
13 *Technology, Haifa 32000 Israel;*

14 *<sup>d</sup>Department of Molecular Microbiology and Biotechnology, Tel Aviv University, Ramat Aviv*  
15 *69978 Israel*

16

17 \*J.S. and S.M. contributed equally to this work.

18 †To whom correspondence should be addressed:

19

Itzhak Mizrahi

20

Tel: (+972)- 8 647 79 859

21

Email: imizrahi@bgu.ac.il

22

23 Running title: Extended cell surface assembly of fibrolytic complex

24

25

## 26 **Abstract**

27 Heterologous display of enzymes on microbial cell surfaces is an extremely  
28 desirable approach, since it enables the engineered microbe to interact directly with the  
29 plant-wall extracellular polysaccharide matrix. In recent years, attempts have been made  
30 to endow non-cellulolytic microbes with genetically engineered cellulolytic capabilities  
31 for improved hydrolysis of lignocellulosic biomass and for advanced probiotics. Thus far,  
32 however, owing to the hurdles of secreting and assembling large, intricate complexes on  
33 the bacterial cell wall, only free cellulases or relatively simple cellulosome assemblies  
34 have been introduced into live bacteria. Here, we employed the “adaptor scaffoldin”  
35 strategy to overcome the low levels of protein displayed on the bacterial cell surface. The  
36 approach mimics natural cellulosome elaborated architectures, thus exploiting the  
37 exponential features of their Lego-like combinatorics. Using this approach, we produced  
38 several bacterial consortia of *Lactobacillus plantarum*, a potent gut microbe which  
39 provides a very robust genetic framework for lignocellulosic degradation. We successfully  
40 engineered surface display of large, fully active self-assembling cellulosomal complexes  
41 containing an unprecedented number of catalytic subunits all produced *in vivo* by the cell-  
42 consortia. Our results demonstrate superior enzyme stability and performance of the  
43 cellulosomal machinery, compared to the equivalent secreted free enzyme system and  
44 high cellulase-to-xylanase ratios proved beneficial for efficient degradation of wheat  
45 straw.

46

## 47 **Importance**

48 The multiple benefits of lactic acid bacteria are well established in health and industry.  
49 Here we present an approach to extensively increase the cell-surface display of proteins  
50 via successive assembly of interactive components. Our findings present a stepping stone  
51 towards proficient engineering of *Lactobacillus plantarum*, a widespread,  
52 environmentally important bacterium and potent microbiome member, for improved  
53 degradation of lignocellulosic biomass and advanced probiotics.  
54

55 **Introduction**

56

57 The plant cell wall is a tough and rigid layer that surrounds the cell to withstand internal  
58 osmotic pressure resulting from the difference in solute concentration between the cell  
59 interior and external water (1). It is composed of various polysaccharides (mostly cellulose  
60 and hemicellulose) and the crosslinked, phenolic polymer lignin. Degradation of the plant  
61 cell wall is performed in nature by various microbial systems that have evolved in order  
62 to utilize its sugars as a main carbon source. The cellulosome (2), first characterized in the  
63 thermophilic anaerobe *Clostridium thermocellum* (3), is a large, highly cellulolytic multi-  
64 enzymatic complex that can be either anchored to the bacterial cell surface (4, 5) or  
65 secreted to the extracellular medium. Cellulosomal complex formation is based on a  
66 unique type of intermodular interaction between its components: the enzymes and the  
67 scaffoldins. Multiple cohesin modules on the scaffoldin and individual dockerin modules  
68 on the enzyme subunits interact in a noncovalent manner with very high affinity that  
69 approaches and surpasses that of antigen-antibody binding (6). The close proximity  
70 between the multiple enzymes serves to enhance synergistic activity (7), and the  
71 carbohydrate-binding module (CBM), usually contained in the scaffoldin subunit, targets  
72 the entire complex to the substrate. When anchored to the bacterial surface, the  
73 cellulosome also contributes to minimal diffusion loss of enzymes and degradation  
74 products.

75 In the past, several studies have reported the fabrication of artificial, chimaeric,  
76 cellulosomal structures, engineered for displayed on the surfaces of various microbial

77 strains, notably *Saccharomyces cerevisiae* (8–11), *Bacillus subtilis* (12, 13), *Clostridium*  
78 *acetobutylicum* (14) and *Lactococcus lactis* (15). For this purpose, designer cellulosome  
79 technology has been employed to mimic the architecture of cellulosome complexes  
80 and/or specifically control their enzyme composition (16–19). One of the major issues of  
81 cell-surface attachment of chimaeric scaffoldins is the low level of surface display that  
82 leads to slow catalysis and low fermentation efficiency (10, 20). The feasibility of  
83 transferring cellulosomal technologies to a bacterium with potential industrial and clinical  
84 applications has been demonstrated recently in *Lactobacillus plantarum* (21–23).  
85 Although this bacterium lacks the native capacity both to degrade cellulosic substrates  
86 and to produce biofuels like ethanol, it is highly tolerant to low pH and ethanol (up to 13%  
87 (v/v)) (24) and has been identified as a main contaminant in biofuel refineries (25).  
88 Therefore, it could also represent an attractive candidate vehicle for consolidated  
89 bioprocessing (CBP) (21, 22). *L. plantarum* is also a member of the human gut microbiome  
90 (26) and additional gut ecosystems (27) and affects host attributes such as mate selection  
91 and growth (28, 29). Moreover, strains belonging to this species were recently shown to  
92 promote juvenile growth and buffer the effect of chronic undernutrition in germ-free  
93 mice (30).

94 Previously, the lignocellulolytic capabilities of engineered *L. plantarum* towards  
95 simple polysaccharides and wheat straw were demonstrated by introducing two key  
96 enzymes, a cellulase and a xylanase, from the thermophilic bacterium *Thermobifida fusca*,  
97 using the previously developed pSIP vectors (31) for efficient secretion of heterologous  
98 proteins (21, 22). The two enzymes were also shown to be displayed directly on the cell

99 surface of cellulosomes, by which the assembly of the enzymes onto a chimaeric  
100 scaffoldin was controlled by specific cohesin-dockerin interactions. The secreted enzymes  
101 were the most active of the three strategies at early times of degradation; but, as  
102 component parts of the surface-attached designer cellulosomes, the enzymes were more  
103 stable in time and achieved similar levels of degradation compared to those of the  
104 secreted enzymes during later times of degradation. In these latter studies, we devised a  
105 novel cell consortium approach in which each engineered *L. plantarum* strain expressed  
106 and secreted different components of the complex to be assembled on the cell wall of a  
107 scaffoldin-expressing strain (21, 22). The labor of producing and secreting the  
108 cellulosomal components was therefore divided among the bacterial community.

109         Nevertheless, due to hurdles of anchoring large scaffoldins on the *L. plantarum*  
110 cell-wall, we were limited in assembling only small numbers of enzymes in the  
111 cellulosomal complex, thus restricting the fiber-degradation capabilities of the  
112 engineered cell consortium. In order to reach superior levels of degradation of the  
113 recalcitrant fiber, and to exploit the potential of the cellulosomal complex, more  
114 enzymatic functions have to be incorporated into the cellulosomal machinery. In order to  
115 overcome these issues, we have, in the current work, mimicked naturally existing  
116 molecular tactics to amplify the inherent enzyme combinatorics and stoichiometric  
117 plasticity used by several cellulosome-producing bacteria (32, 33). This approach allows  
118 the expression of large, stable and active self-assembling protein complexes on the  
119 bacterial cells and may provide an effective strategy to achieve enhanced cell-surface  
120 display of the engineered enzymes thereby expanding the lignocellulolytic potential in *L.*

121 *plantarum*.

## 122 **Results**

123 **Engineering of fully active mesophilic enzymes for assembly of cellulosomal structures**  
124 **on the *L. plantarum* cell wall.** Since the host ‘vehicle’ for our study, *L. plantarum*, is a  
125 mesophile, we searched for appropriate enzymes derived from mesophilic bacteria to be  
126 used as designer cellulosome components for surface display. Our recent involvement in  
127 genomic sequencing of the mesophilic cellulolytic bacterium, *C. papyrosolvens* (34),  
128 provided a wealth of potentially compatible enzymes for our study.

129 The *C. papyrosolvens* enzymes, selected for heterologous secretion in *L. plantarum*  
130 destined for self-assembly into active designer cellulosomes on the *L. plantarum* cell  
131 surface, are shown schematically in Fig. 1A. *C. papyrosolvens* exhibits strong genome  
132 homology with the closely related mesophile, *Clostridium cellulolyticum*, which was  
133 demonstrated previously to possess highly efficient polysaccharide-degrading enzymes,  
134 both in the context of *in vitro* designer cellulosomes (17, 35) and for yeast- or bacterial-  
135 based CBP (14, 36). Two putative *C. papyrosolvens* cellulases, GH5 and GH9, were selected  
136 on the basis of their homology with the two known synergistic cellulases from *C.*  
137 *cellulolyticum*, i.e., the processive endoglucanase Cel9G and the Cel5A endoglucanase  
138 (17). Two putative xylanases were also selected: one from the GH11 family, homologous  
139 to *C. cellulolyticum* Xyn11A, and another from the GH10 family, homologous to *C.*  
140 *cellulolyticum* Xyn10A. Both of the *C. cellulolyticum* enzymes were characterized as  
141 efficient xylanases (37, 38).

142 The cohesin-dockerin assembly is species-specific (39, 40). Therefore, in order to

143 control the composition and architecture of the desired designer cellulosomes, each  
144 enzyme was designed to contain a dockerin derived from a distinct bacterial species that  
145 will match a specific cohesin on the chimaeric scaffoldin (16). The chimaeric enzymes  
146 were thus modified by replacing the original *C. papyrosolvens* dockerin module (that  
147 share the same binding specificity) with dockerins from other bacterial species, resulting  
148 in enzymes with different cohesin-binding specificities.

149 The hydrolytic activity of each of the five purified recombinant chimaeric enzymes  
150 from *C. papyrosolvens* was compared to that of the corresponding recombinant wild-type  
151 enzyme, all produced in *Escherichia coli* (Supplementary materials: Fig. S1). The wild-type  
152 enzymes and their respective recombinant chimaeras were fully active on all cellulosic  
153 substrates or on xylan.

154

155 **Newly designed recombinant synthetic scaffoldins.** In order to increase the  
156 combinatorics of the synthetic cellulosomal machinery, we have mimicked the existing  
157 natural microbial “adaptor-scaffoldin” approach into heterogeneous bacterial cells (36,  
158 41, 42). In this approach, several scaffoldins are assembled together through mediation  
159 via adaptor scaffoldin(s) thereby increasing the number of enzymatic components in the  
160 cellulosomal complex (Fig. 1D). We designed two types of adaptor scaffoldins for enzyme  
161 integration (Fig. 1B): one type, Adaptor-1, contains the two cohesin modules that bind the  
162 two dockerin-containing cellulases, and the second, Adaptor-2, contains two cohesin  
163 modules that incorporate the two dockerin-containing xylanases. In addition to the 2  
164 enzyme-integrating cohesins, each adaptor scaffoldin contains a substrate-targeting CBM

165 and a type II or type III dockerin, respectively, for interaction with the cell surface-  
166 anchoring scaffoldin (42).

167 As mentioned above, one of the advantages of using the adaptor-scaffoldin  
168 approach is that it amplifies the combinatoric and stoichiometric possibilities for enzyme  
169 integration. In order to explore the combinatorial possibilities and to increment  
170 methodically the number of enzymes integrated into the complex, we created 5 different  
171 types of anchoring scaffoldins, as represented in Fig. 1C, that enable the insertion of up  
172 to 8 enzymes into the displayed designer cellulosomes. All of the anchoring scaffoldins  
173 contain a sortase signal motif for covalent attachment to the cell-surface via a resident *L.*  
174 *plantarum* sortase (43). While Anc-1 is composed of four different type I cohesin modules  
175 that directly interact with the four dockerin-bearing enzymes (the two cellulases and the  
176 two xylanases); Anc-2, Anc-3 and Anc-4 possess several copies of type II and III cohesins  
177 with different specificities. This setup of divergent specificities also allows us to analyze  
178 the influence of stoichiometry of the xylanases versus the cellulases on plant fiber  
179 degradation by enabling the attachment of either one or two copies of the cellulase-  
180 bearing adaptor scaffoldin (Adaptor-1) or one or two copies of the xylanase-bearing  
181 adaptor scaffoldin (Adaptor-2). An example of the various cell-surface-displayed  
182 cellulosome assemblies produced by the different cell consortia is shown in Fig. 1D.

183 In order to examine the binding abilities of our engineered complexes, the two  
184 adaptor scaffoldins and five anchoring scaffoldins were initially purified recombinantly in  
185 *E. coli*. The respective binding specificities of the cohesin and dockerin modules of both  
186 the purified adaptor scaffoldins and anchoring scaffoldins were examined by performing

187 native gel electrophoresis, and each recombinant protein was shown to interact  
188 selectively with its expected partner (see example in Fig. S2).

189

### 190 **Secretion of active recombinant *C. papyrosolvens* mesophilic enzymes by *L. plantarum***

191 The secretion and functionality of enzymes by *L. plantarum* were analyzed by comparing  
192 the enzymatic activity of concentrated culture supernatant fluids from transformed  
193 lactobacilli with that of the pure recombinant proteins from *E. coli* (Fig. S3). The two  
194 xylanases actively degraded xylan, and their concentration was thus estimated (Fig. S3A  
195 and B, Table 1). The two cellulases were not properly secreted using leader peptide  
196 Lp3050 (data not shown). We therefore selected an alternative leader peptide (Lp2588),  
197 which was also reported as an efficient candidate for secretion of foreign proteins in *L.*  
198 *plantarum* (31). The cellulase activities observed in Figs. S3C and D served to estimate the  
199 concentrations of the respective proteins (Table 1) (21). In parallel, we verified the  
200 presence of full-length recombinant enzymes and their ability to properly bind their  
201 respective cohesin modules by Far Western blot analysis (Supplementary materials: Fig.  
202 S4).

203

204 ***L. plantarum* secretes and anchors active chimaeric scaffoldins** After examining the  
205 proper functionality and integrity of the enzymes to function within the cellulosomal  
206 complex, we examined the expression of anchoring and adaptor scaffoldins in *L.*  
207 *plantarum*, which will integrate the enzymes to form the desired elaborate cellulosomal  
208 structures.

209           The secretion of the adaptor scaffoldins and their functionality were analyzed  
210 using an ELISA-based binding assay by comparing the binding properties of the pure  
211 recombinant proteins (produced in *E. coli*) to culture supernatants from transformed  
212 lactobacilli. We found that the adaptor scaffoldins were properly secreted into the  
213 extracellular medium and exhibited the expected cohesin-dockerin binding capacities  
214 (Supplementary materials Fig. S5). In addition, in Fig. 2 we can observe that the binding  
215 properties of the adaptor scaffoldins attached to the anchoring scaffoldins are functional.  
216 The presence of full-length adaptor scaffoldins was also verified by Western blot analysis  
217 (Supplementary materials Fig. S4). The anchoring and functionality of the chimaeric  
218 scaffoldins were also analyzed by ELISA-based binding assay by comparing the binding  
219 properties of pure proteins (xylanase tag fused to the different dockerins) to washed  
220 whole bacterial cells from transformed lactobacilli (Supplementary materials Fig. S6). We  
221 observed that anchoring scaffoldins composed of two and three cohesins (Anc-2, Anc-3a  
222 and Anc-3b) were attached and fully functional on the *L. plantarum* cell surface. Both  
223 cohesin/dockerin pairs, appeared to enable comparably high interaction events  
224 (Supplementary materials Fig. S6). On the other hand, anchoring scaffoldins composed of  
225 4 cohesins (Anc-1 and Anc-4) did not exhibit full binding abilities, as they showed  
226 insufficient binding for two of their cohesins (Fig. 2 and Supplementary materials Fig. S6).  
227 In both cases, the cohesins adjacent to the anchoring signal motif were not functional.  
228 This result emphasizes the importance of using the adaptor scaffoldin strategy in this  
229 system, since incorporation of four different dockerin-bearing enzymes extends the  
230 number of catalytic subunits, and this would not be achieved by using a single scaffoldin

231 directly anchored onto the *L. plantarum* cell surface.

232 ELISA-based binding assays both for adaptor and anchoring scaffoldins also served  
233 to evaluate the quantity of secreted or anchored proteins of the different transformed  
234 strains of *L. plantarum* by using standard curves of known concentrations of pure proteins  
235 (Table 1).

236

237 ***L. plantarum* cells displaying synthetic elaborate cellulosomal machinery show**  
238 **superior performance over secreted enzymes and simple synthetic cellulosome**  
239 **strategies.** As we reported previously (22), the cell consortia approach is a highly efficient  
240 way for assembling large complexes on bacterial cell walls. In this approach, the effort of  
241 producing and secreting the cellulosomal complex is divided among several strains – each  
242 secreting a different cellulosomal component of the cellulosome, thereby enabling its  
243 combined assembly on the cell wall of the anchored scaffoldin-containing strain. In  
244 addition, since we obtained relatively large differences in the quantity of  
245 secreted/anchored proteins, the flexibility provided by the cell consortium approach is  
246 essential to control the production of cellulosomal complexes, which stoichiometric  
247 amounts of the relevant components.

248 Here, we examined the ability of the elaborate cellulosomal machineries to degrade  
249 natural plant fiber material (pre-treated wheat straw) as well as to compare their action  
250 to that of the free secreted enzyme approach. To this end, six different types of microbial  
251 consortia were examined as detailed in Fig. 3B. Using these consortia, we experimented  
252 with different stoichiometries of the cellulosomal and secreted enzyme components (Fig.

253 3A).

254 Microbial consortia examined in this work produce either the free enzymes or the  
255 surface-displayed designer cellulosomes, and the bacterial cells would directly consume  
256 the sugars produced by their different enzymatic arrangements. Hence, in order to  
257 elucidate the portion of sugars that is consumed by our microbial consortia we performed  
258 *in vitro* enzymatic hydrolysis with enzymes or assembled designer cellulosomes produced  
259 and purified from *E. coli* (Fig. 3C), in order to determine the level of soluble sugar  
260 production in the absence of *L. plantarum* cells. Indeed, as presented in Fig. 3C, we  
261 observed higher amounts of sugars produced by the enzymatic mixtures as opposed to  
262 the residual sugars measured after incubation with the microbial consortia (Fig. 3A). In  
263 addition, we could see from both Figs. 3A and C that the designer cellulosomes  
264 consistently outperformed their respective free enzyme counterparts (bars 1, 2 and 3  
265 compared to 4, 5 and 6).

266 In Fig. 3C, the comparative degradation of pre-treated wheat straw by the *in vitro*-  
267 applied enzymes and designer cellulosomes revealed that designer cellulosomes  
268 comprising two copies of the cellulases (bar 2) was the best-performing enzymatic  
269 complex. By comparison, in Fig. 3A, the soluble (residual) sugar measurements reflected  
270 the amount of sugars that were not consumed by the *L. plantarum* consortia. We then  
271 further evaluated the kinetics of the reaction were also evaluated using microbial  
272 consortia, which revealed the continued activity of the anchored designer cellulosomes  
273 until 96 h, whereas the free enzymes failed to produce additional soluble sugars after 48h  
274 (Fig. S7). Further analysis of unconsumed released sugars from pre-treated wheat straw

275 degradation using high performance anionic exchange chromatographic (Table S1),  
276 revealed high amounts of xylan degradation products (mainly xylobiose and xylotriose),  
277 suggesting that *L. plantarum* could not assimilate these carbon sources.

278

## 279 **Discussion**

280 In this study, we used the adaptor scaffoldin strategy for assembly of elaborate  
281 cellulosomal structures (36, 41, 42) on the cell surface of *L. plantarum* for both  
282 augmenting cell-surface display and improving its fiber-degrading potential. For this  
283 purpose, the use of potent enzymes originating from a mesophilic cellulosome-producing  
284 species, *Clostridium papyrosolvens*, is well-suited for expression in the gut ecosystem (a  
285 common *L. plantarum* habitat). Here, all the cellulosomal components were produced *in*  
286 *vivo* by the cell-consortia and not supplemented *ex vivo* as previously reported (36, 41).

287 Cellulosomal complexes have attracted increased interest in recent years, since  
288 lignocellulosic biomass represents a particularly abundant resource for conversion into  
289 fermentable sugars, suitable for production of biofuels (44). We recently reported the  
290 successful incorporation of simple divalent designer cellulosome components onto the  
291 cell wall of *Lactobacillus plantarum* (22), an attractive candidate for consolidated  
292 bioprocessing (22, 45, 46). Here, the adaptor scaffoldin strategy was demonstrated to be  
293 an effective approach (i) for increasing the number of catalytic units in the cellulosome  
294 complex displayed on the cell-surface, thereby bypassing the relatively low cell-surface  
295 display of scaffoldins, and (ii) for achieving high binding capacities of the bacterial cell to  
296 the substrate.

297           In this work, we produced elaborate cellulosomal complexes by employing a cell-  
298 consortium approach, whereby each recombinant strain of *L. plantarum* expresses an  
299 individual cellulosomal component (secreted to the extracellular medium or anchored to  
300 the bacterial cell surface). A total of four chimaeric cellulosomal enzymes (cellulases and  
301 xylanases derived from *C. papyrosolvens*) and two adaptor scaffoldins were functionally  
302 secreted into the extracellular media. In addition, five different types of anchoring  
303 scaffoldins were tested for their ability to properly interact subsequently with the  
304 secreted cellulosomal elements. By composing various co-cultures of recombinant  
305 bacteria expressing the heterologous proteins separately, we were able to attach up to  
306 three adaptor scaffoldins to the anchoring scaffoldins for potential display of up to six  
307 catalytic subunits on the cell surface. Using co-cultures offers the advantage that the  
308 composition of the surface-anchored designer cellulosome, produced by an appropriate  
309 cell consortium, can be easily controlled by adjusting the ratio of each cell type during  
310 inoculation. It was also demonstrated that co-cultures of recombinant bacteria expressing  
311 heterologous proteins did not affect the initial ratio of the strains and therefore did not  
312 affect the ratio of proteins expressed (21). The cell-consortium approach decreases  
313 considerably the burden of the cellular machinery of each strain, thereby maximizing their  
314 ability to grow and to express the various cellulosomal components. In nature, this type  
315 of spatial differentiation strategy is commonly employed by prokaryotic species in a given  
316 ecosystem, which results in a collaboration among the different cell types to achieve a  
317 unique objective from which they will all benefit (47).

318           The variety of anchoring and adaptor scaffoldins allowed us to examine the

319 importance of ratios among the different enzymatic components in order to obtain  
320 efficient substrate degradation. The highest levels of degradation in the present studies  
321 were obtained when a trivalent anchoring scaffoldin enabled attachment to the cell  
322 surface of three adaptor scaffoldins incorporating a total of four cellulases (2 copies of  
323 Adaptor 1) and two xylanases (single copy of Adaptor 2) (see Fig. 3C, Bar 2). This enzymatic  
324 combination was also optimal among purified free enzymes (Fig. 3C, Bar 5). Since the  
325 kinetics of xylan removal by the employed xylanases is much more higher than the slower  
326 cellulose degradation by cellulases used in this study (Fig. S1), it would be therefore logical  
327 that a higher cellulase/xylanase ratio would be required for optimized wheat straw  
328 deconstruction.

329         We observed here that the cellulosome paradigm was more efficient than the  
330 secreted free-enzyme approach and that elaborate cellulosome structures (consortia 2  
331 and 3) conferred high stability to the catalytic subunits (Table 2) and high cellulose-  
332 binding abilities to the bacterial cells (Table 3). The stability of the enzymes seems to be  
333 a key parameter in terms of enzymatic efficiency. At later cultivation times (above 48 h)  
334 the anchoring paradigm appears more advantageous than the secreted free enzyme  
335 paradigm for the same enzymatic composition (Fig. S7). This corresponds to the decrease  
336 in stability of the secreted cellulases (Table 2), whereas the anchored enzymes remain  
337 fully active. While the cellulosomal machinery is considered to induce synergistic activity  
338 among the catalytic modules by their close proximity within the complex (5, 7), the  
339 present study as well as others (48, 49) strongly support the importance of the stability  
340 conferred upon the enzymes by the scaffoldin subunit.

341           The ability of the bacteria to utilize the wheat straw substrate as the sole carbon  
342 source was assessed on a chemically defined medium. However, wheat straw failed to  
343 sustain growth of either the wild-type bacteria or the consortium 2 that produces the  
344 highest amount of sugars (data not shown). We further examined the minimal amount  
345 of sugar required to sustain growth by growing wild-type *L. plantarum* cells on either  
346 glucose, cellobiose, xylose or xylobiose. No growth was observed on pure xylose and  
347 xylobiose while the minimal concentration that sustained growth was 0.2% glucose (~11  
348 mM) or 0.2% cellobiose (~5.5 mM) on chemically defined medium (CDM) (Fig. S8). The  
349 sugars produced by the best-performing cellulosomal machinery (Fig.3C, bar 2) was about  
350 17 mM of a mixture of soluble sugar products, some of which are not utilizable, and about  
351 4 mM of unconsumed sugars (Fig.3A, bar 2). The lack of growth suggests that the amount  
352 and type of sugars produced by the consortia are the limiting factor for growth  
353 sustainability. To bridge this gap in future studies, we will screen for additional highly  
354 expressed cellulases, in order to generate higher production of sugars that can be  
355 assimilated. In addition, it is important to fine-tune the amount and/or types of xylanases,  
356 which, on the one hand, serve to remove the embedded xylan that prevents physical  
357 access of the cellulases to the cellulose, but, on the other, will produce sugars that are  
358 not consumed by the *L. plantarum* cells. The data in Table S2 suggests that xylose may be  
359 assimilated by the cells, since low concentrations of xylose were detected in the presence  
360 of *L. plantarum*. The complete genome sequence of *L. plantarum* WCFS1 indeed suggests  
361 the presence of genes involved in xylose transport but genes for D-xylose isomerase and  
362 D-xylose kinase were not detected (50), indicating that xylose cannot be fermented.

363 Indeed, effective xylose transport was also demonstrated for strain 3NSH, but xylose was  
364 not metabolized in these studies (51). Therefore, further research should consider the  
365 implementation of xylose assimilation genes in strain WCSF1 as for strain NCIMB 8826  
366 (52). Alternative explanations for the lack of bacterial growth by the cell consortia should  
367 be examined in future studies, such as the potential release of cellulase inhibitors by  
368 xylanase action (53).

369         Within the context of gut microbiome ecosystems, the xylan degradation products  
370 produced by the cell consortia developed in this work could also benefit the overall  
371 microbial community. As a potent gut microbe, the engineering of *L. plantarum* towards  
372 fiber degradation could be highly beneficial for clinical applications, such as probiotics  
373 (26). Indeed, by enabling this bacterium to degrade plant fiber, we potentially increase its  
374 fitness in the gut by extending its status in the ecosystem, which will allow it to better  
375 persist as a probiotic organism. Furthermore, the augmented cell-surface display  
376 conferred by the adaptor scaffoldin strategy could serve to promote higher efficiency of  
377 mucosal vaccines, based on bacteria as delivery vehicles (54).

378

## 379 **Material and Methods**

380 All the experiments have been replicated three times in triplicate, and the data served to  
381 perform the statistical calculations in the relevant figures and tables.

382         **Cloning.** All recombinant proteins employed in this study (see representation in  
383 Figure 1) were first cloned into pET28a plasmids and designed to contain a His-tag for  
384 subsequent purification by standard restriction-based cloning procedures (55). The

385 recombinant enzymes from *C. papyrosolvens* were produced by replacing their native  
386 dockerins with dockerins of different specificities using respective genomic DNA: 5-g was  
387 obtained by fusing the catalytic module of *C. papyrosolvens* GH5 (GenBank: EPR12097.1)  
388 to a dockerin from *Archeoglobus fulgidus* (Orf2375), 9-b was obtained by fusing the  
389 catalytic module of *C. papyrosolvens* GH9 (GenBank: EPR13542.1) to a dockerin of  
390 *Bacteroides cellulosolvens* (ScaA), 10-t was obtained by fusing the catalytic module of *C.*  
391 *papyrosolvens* GH10 (GenBank: EPR14039.1) to a dockerin of *C. thermocellum* (Cel48S)  
392 and 11-a was obtained by fusing the catalytic module of *C. papyrosolvens* GH11 (GenBank:  
393 EPR13563.1) to a dockerin of *Acetivibrio cellulolyticus* (ScaB).

394 The adaptor scaffoldins Adaptor·1 and Adaptor·2 were obtained by fusing  
395 previously employed bivalent scaffoldins (19) to a type II dockerin from *C. thermocellum*  
396 (CipA) for Adaptor·1 and to a type III dockerin from *Ruminococcus flavefaciens* 17 (ScaB)  
397 for Adaptor·2.

398 The anchoring scaffoldins Anc·2, Anc·3a, Anc·3b and Anc·4 were obtained by fusing  
399 one or two type II cohesins from *C. thermocellum* (OlpB) to one or two type III cohesins  
400 from *R. flavefaciens* 17 (ScaE), as designated in Figure 1.

401 The enzymes and the genes coding for the two adaptor scaffoldins were introduced  
402 into *L. plantarum* using the previously employed pSIP vectors for efficient  
403 secretion/attachment of heterologous proteins (21, 22) using the leader peptide (Lp)  
404 Lp3050 via pLp\_3050sAmy, by replacing the amylase gene in these plasmids by an  
405 appropriately amplified gene fragment (31). As the five different anchoring scaffoldins  
406 (Anc·1, Anc·2, Anc·3a, Anc·3b and Anc·4) are to be integrated into the bacterial cell wall,

407 we fused them into the potent cell wall anchor (cwa) anchoring signal cwa2 (22) via the  
408 modular pLp\_0373sOFA anchoring plasmids (56).

409 To amplify DNA fragments by PCR for cloning, T-Gradient device (Biometra,  
410 Germany) was used. The PCR was performed in 50 µl reaction mixtures.

411 For short PCR products (up to 500 base pairs), PCR ready mix (Abgen, Epsom, Surrey,  
412 UK) was employed. For longer PCR fragments, PCRs were performed using Phusion high-  
413 fidelity DNA polymerase F530-S (New England BioLabs, Inc.). Primers were added to a  
414 final concentration of 0.5 µM. PCR was programmed according to each manufacturer's  
415 instructions. Primers are listed in Table S2 of the supplementary materials.

416 **Protein expression and purification from *Escherichia coli*.** Recombinant proteins  
417 were expressed in *E. coli* BL21 (DE3) and purified as described earlier (18, 42).

418 **Protein expression in *L. plantarum*.** The methodology described in Morais et al was  
419 followed (22). For the consortia experiments, strains producing either cellulase, xylanase,  
420 adaptor or anchoring scaffoldins, were mixed at stoichiometric molar ratios for the  
421 enzyme/scaffoldin, and scaffoldin/scaffoldin interactions and then grown on MRS (as  
422 prepared by BD Difco™ without protease peptone) supplemented with 40 mM CaCl<sub>2</sub>.

423 **Western and Far-Western blotting of *L. plantarum* secreted proteins.** The  
424 methodology described in Morais et al was followed (22) for Western Blot experiments  
425 (Fig. S4, E and F). In Far-Western Blot (Fig. S4, A, B, C and D), an interaction step was  
426 included after blocking. Binding interactions with the blotted proteins were assayed with  
427 tagged fusions of specific cohesins fused to the CBM3a module (from the *C. thermocellum*  
428 scaffoldin) (CBM-Coh) (57, 58). Specific rabbit antibody against the fused tag (CBM)

429 diluted at 1:3000 (58, 59) was used as the primary antibody. The Far Western Blot  
430 experiments served here to verify both the presence of the full-length dockerin-bearing  
431 enzymes and their ability to bind their respective cohesins.

432 **ELISA binding assay.** The methodology described in Barak et al was followed (57)  
433 with the following modification. MaxiSorp ELISA plates (Nunc A/S, Roskilde, Denmark)  
434 were coated overnight at 4°C with 1 µg/ml of either the specific dockerin fused to  
435 xylanase T6 from *Geobacillus stearothermophilus* (Xyn-Doc) or the CBM-Coh (100 µl/well)  
436 in 0.1 M sodium carbonate (pH 9). After the blocking step, incremental dilutions of either  
437 *L. plantarum* washed whole cells, concentrated supernatant fluids (OD<sub>600</sub>= 1) or 100 ng/ml  
438 of purified recombinant proteins in blocking buffer were added. Specific rabbit antibody,  
439 raised against either the CBM diluted at 1:3000 in blocking buffer or the type II cohesin  
440 from *C. thermocellum* (1:10000 dilution), was used as primary antibody.

441 **Enzymatic activity on pre-treated wheat straw degradation.** Prior to enzymatic  
442 assay, culture supernatant fluids (for secreted proteins) were concentrated using Amicon  
443 centrifugal filters with a 30-kDa cut-off (Millipore, Molsheim, France) and washed with  
444 Tris Buffer Saline (TBS x10: 80 g NaCl, 2 g KCl, 30 g Tris, ddw to 1L, adjust pH to 7.4 with  
445 HCl 32%) containing 40 mM CaCl<sub>2</sub>; cells (for anchored designer cellulosomes) were  
446 washed with TBS containing 1% Triton X-100 by centrifugation and resuspension to  
447 eliminate the sugars present in the MRS medium. Hatched wheat straw, pre-treated with  
448 12% sodium hypochlorite, was prepared as described before (18). This type of  
449 pretreatment selectively removes lignin from the biomass, leaving the hemicellulose  
450 fraction largely intact. A typical assay mixture consisted of either washed whole cells or

451 concentrated supernatant fluids from *L. plantarum* at specified concentrations, applied  
452 to a suspension of 40 g/liter pre-treated wheat straw in the relevant specified reaction  
453 volume (50 mM citrate buffer [pH 6.0], 12 mM CaCl<sub>2</sub>, 2 mM EDTA). Reactions were  
454 incubated at 37°C under shaking. The total amount of sugars released was determined  
455 using the dinitrosalicylic acid (DNS) assay as described previously (42, 60).

456 When pure proteins or designer cellulosomes were employed (Fig. 3C), similar  
457 conditions were used with a stoichiometric concentration of enzymes (and scaffoldins),  
458 whereby the anchoring scaffoldin was set at 12 nM. The designer cellulosomes were  
459 allowed to assemble for 3 h at room temperature with all the enzymatic assay  
460 components except the wheat straw substrate. Upon addition of the wheat straw, the  
461 enzymatic reaction mixture was incubated for 96 h at 37°C under shaking.

462 **Sugar analysis.** Sugar content was analyzed using a high-performance anion-  
463 exchange chromatography (HPAEC) system equipped with a PA1 column (Dionex,  
464 Sunnyvale, CA). Supernatants of the reaction mixtures obtained after centrifugation were  
465 loaded onto the PA1 column, and eluted with 200 mM NaOH (flow rate of 1 ml/min). At  
466 first, standards consisting of pure arabinose, xylose, xylobiose, xylotriose, glucose,  
467 cellobiose, and cellotriose were loaded separately to determine elution time and peak  
468 areas as a function of the sugar concentration. Sugars present in blank were deducted in  
469 all the samples.

470 **Stability assay.** The stability of the enzymatic combination at 37°C was  
471 determined by incubating the described consortia (at 3 nM for each enzyme) without  
472 substrate over a 48-h period at 37°C. The residual enzymatic activity was calculated as the

473 relative activity of the consortium incubated at 37°C compared to that of the anchored  
474 consortium (washed whole cells) or secreted consortium (concentrated supernatant  
475 fluids) that was directly introduced to the substrate (with no incubation period), on  
476 carboxymethyl cellulose (CMC) or beechwood xylan for a period of 2 hours at 37°C.

477 **Adherence/turbidity assay.** Wild-type *L. plantarum* bacteria or consortia of  
478 transformed strains were grown with inducer until  $OD_{600}=1$ . A volume of 1 mL of the  
479 cultures was then subjected to interaction with 30 mg of Avicel for 1h at 4°C in TBS  
480 supplemented with 40 mM  $CaCl_2$ . Gentle centrifugation (about 1 min at 1000 rpm) was  
481 then performed to separate the Avicel substrate. The absorbance at  $OD_{600}$  was then  
482 verified, using MRS medium supplemented with Avicel under the same conditions as a  
483 blank without bacterial cells. The difference in absorbance at  $OD_{600}$  reflects the adhesion  
484 of the cells to cellulose.

485 **Bacterial growth.** A chemically defined medium (CDM) as developed by Wegkamp  
486 et al (61) was prepared with 20 g/l pre-treated wheat straw. In parallel, consortium 2 or  
487 the wild-type bacteria were cultured in MRS without protease peptone as described  
488 above. Cells were harvested, washed twice in 10 ml 0.85% NaCl and 10 mM  $CaCl_2$ , and the  
489 washed cells served as an inoculum of the CDM containing wheat straw as carbon source.  
490 The medium was supplemented with pSIP inducer, 10 mM  $CaCl_2$ , and erythromycin in the  
491 case of consortium 2. Growth at 37°C under agitation (200 rpm) was followed for a week  
492 by measuring the OD at 600 nm of the supernatant culture after the wheat straw  
493 precipitated (5 min). Growth of the wild-type bacteria was assessed on CDM  
494 supplemented with 0 to 1% of either cellobiose, glucose, xylose or xylobiose.

495

496 **Funding information**

497           The research was supported by grants from the Israel Science Foundation (No.  
498 1313/13 to IM and 1349/13 to EAB), by the Israeli Chief Scientist Ministry of Agriculture  
499 and Rural Development Fund (No. 362-0426) to EAB and IM, by the Israeli Chief Scientist  
500 Ministry of Science Foundation (No.3-10880) to EAB and IM, by the European Research  
501 Council (No. 640384) to IM, and by the United States-Israel Binational Science Foundation  
502 (BSF). The authors appreciate the support of the European Union, CellulosomePlus (No.  
503 604530) and European Union Horizon 2020: Waste2Fuels. EAB is the incumbent of The  
504 Maynard I. and Elaine Wishner Chair of Bio-organic Chemistry.

505

## 506 REFERENCES

- 507 1. Doblin MS, Pettolino F, Bacic A. 2010. Evans Review : Plant cell walls: the skeleton of the  
508 plant world. *Funct Plant Biol* 37:357.
- 509 2. Artzi L, Bayer EA, Moraïs S. 2016. Cellulosomes: bacterial nanomachines for dismantling  
510 plant polysaccharides. *Nat Rev Microbiol*.
- 511 3. Lamed R, Setter E, Bayer EA. 1983. Characterization of a cellulose-binding, cellulase-  
512 containing complex in *Clostridium thermocellum*. *J Bacteriol* 156:828–36.
- 513 4. Shoham Y, Lamed R, Bayer EA. 1999. The cellulosome concept as an efficient microbial  
514 strategy for the degradation of insoluble polysaccharides. *Trends Microbiol* 7:275–281.
- 515 5. Bayer EA, Belaich J-P, Shoham Y, Lamed R. 2004. The Cellulosomes: Multienzyme Machines  
516 For Degradation Of Plant Cell Wall Polysaccharides. *Annu Rev Microbiol* 58:521–554.
- 517 6. Adams JJ, Pal G, Jia Z, Smith SP. 2006. Mechanism of bacterial cell-surface attachment  
518 revealed by the structure of cellulosomal type II cohesin-dockerin complex. *Proc Natl Acad*  
519 *Sci U S A* 103:305–310.
- 520 7. Bayer EA, Setter E, Lamed R. 1985. Organization and distribution of the cellulosome in  
521 *Clostridium thermocellum*. *J Bacteriol* 163:552–9.
- 522 8. Tsai S-L, Oh J, Singh S, Chen R, Chen W. 2009. Functional assembly of minicellulosomes on  
523 the *Saccharomyces cerevisiae* cell surface for cellulose hydrolysis and ethanol production.  
524 *Appl Environ Microbiol* 75:6087–93.
- 525 9. Tsai S-L, Goyal G, Chen W. 2010. Surface display of a functional minicellulosome by  
526 intracellular complementation using a synthetic yeast consortium and its application to  
527 cellulose hydrolysis and ethanol production. *Appl Environ Microbiol* 76:7514–20.
- 528 10. Wen F, Sun J, Zhao H. 2010. Yeast surface display of trifunctional minicellulosomes for  
529 simultaneous Saccharification and fermentation of cellulose to ethanol. *Appl Environ*

- 530 Microbiol 76:1251–1260.
- 531 11. Lilly M, Fierobe H-P, van Zyl WH, Volschenk H. 2009. Heterologous expression of a  
532 *Clostridium* minicellulosome in *Saccharomyces cerevisiae*. FEMS Yeast Res 9:1236–49.
- 533 12. You C, Zhang X-Z, Sathitsuksanoh N, Lynd LR, Zhang Y-HP. 2012. Enhanced microbial  
534 utilization of recalcitrant cellulose by an ex vivo cellulosome-microbe complex. Appl  
535 Environ Microbiol 78:1437–44.
- 536 13. Anderson TD, Robson S a., Jiang XW, Malmirchegini GR, Fierobe HP, Lazazzera BA, Clubb  
537 RT. 2011. Assembly of minicellulosomes on the surface of *Bacillus subtilis*. Appl Environ  
538 Microbiol 77:4849–4858.
- 539 14. Willson BJ, Kovács K, Wilding-Steele T, Markus R, Winzer K, Minton NP. 2016. Production  
540 of a functional cell wall-anchored minicellulosome by recombinant *Clostridium*  
541 *acetobutylicum* ATCC 824. Biotechnol Biofuels 9:109.
- 542 15. Wieczorek AS, Martin VJJ. 2010. Engineering the cell surface display of cohesins for  
543 assembly of cellulosome-inspired enzyme complexes on *Lactococcus lactis*. Microb Cell  
544 Fact 9:69.
- 545 16. Bayer EA, Morag E, Lamed R. 1994. The cellulosome — A treasure-trove for biotechnology.  
546 Trends Biotechnol 12:378–386.
- 547 17. Fierobe H, Mingardon F, Mechaly A, Be A, Rincon MT, Lamed R, Tardif C, Be J, Bayer EA.  
548 2005. Action of Designer Cellulosomes on Homogeneous Versus Complex substrates  
549 280:16325–16334.
- 550 18. Morais S, Morag E, Barak Y, Goldman D, Hadar Y, Lamed R, Shoham Y, Wilson DB, Bayer  
551 EA. 2012. Deconstruction of lignocellulose into soluble sugars by native and designer  
552 cellulosomes. MBio 3:1–11.
- 553 19. Morais S, Barak Y, Caspi J, Hadar Y, Lamed R, Shoham Y, Wilson DB, Bayer EA. 2010.

- 554 Cellulase-xylanase synergy in designer cellulosomes for enhanced degradation of a  
555 complex cellulosic substrate. *MBio* 1:e00285-10.
- 556 20. Huang GL, Anderson TD, Clubb RT. 2013. Engineering microbial surfaces to degrade  
557 lignocellulosic biomass. *Bioengineered* 5:1–11.
- 558 21. Morais S, Shterzer N, Grinberg IR, Mathiesen G, Eijsink VGH, Axelsson L, Lamed R, Bayer E  
559 a., Mizrahi I. 2013. Establishment of a simple *Lactobacillus plantarum* cell consortium for  
560 cellulase-xylanase synergistic interactions. *Appl Environ Microbiol* 79:5242–5249.
- 561 22. Morais S, Shterzer N, Lamed R, Bayer EA, Mizrahi I. 2014. A combined cell-consortium  
562 approach for lignocellulose degradation by specialized *Lactobacillus plantarum* cells.  
563 *Biotechnol Biofuels* 7:112.
- 564 23. Mazzoli R, Bosco F, Mizrahi I, Bayer EA, Pessione E. 2014. Towards lactic acid bacteria-  
565 based biorefineries. *Biotechnol Adv* 32:1216–1236.
- 566 24. G-Alegría E, López I, Ruiz JI, Sáenz J, Fernández E, Zarazaga M, Dizy M, Torres C, Ruiz-Larrea  
567 F. 2004. High tolerance of wild *Lactobacillus plantarum* and *Oenococcus oeni* strains to  
568 lyophilisation and stress environmental conditions of acid pH and ethanol. *FEMS Microbiol*  
569 *Lett* 230:53–61.
- 570 25. Lucena BT, dos Santos BM, Moreira JL, Moreira APB, Nunes AC, Azevedo V, Miyoshi A,  
571 Thompson FL, de Morais M. 2010. Diversity of lactic acid bacteria of the bioethanol  
572 process. *BMC Microbiol* 10:298.
- 573 26. Walter J. 2008. Ecological role of *Lactobacilli* in the gastrointestinal tract : implications for  
574 fundamental and biomedical research. *Appl Env Microbiol* 74:4985–4996.
- 575 27. Martino ME, Bayjanov JR, Caffrey BE, Wels M, Joncour P, Hughes S, Gillet B, Kleerebezem  
576 M, Lyon CB. 2016. Nomadic lifestyle of *Lactobacillus plantarum* revealed by comparative  
577 genomics of 54 strains isolated from different habitats. *Env Microbiol* 18:4974–4989.

- 578 28. Storelli G, Defaye A, Erkosar B, Hols P, Royet J, Leulier F. 2017. *Lactobacillus plantarum*  
579 Promotes *Drosophila* Systemic Growth by Modulating Hormonal Signals through TOR-  
580 Dependent Nutrient Sensing. *Cell Metab* 14:403–414.
- 581 29. Sharon G, Segal D, Ringo JM, Hefetz A, Zilber-Rosenberg I, Rosenberg E. 2010. Commensal  
582 bacteria play a role in mating preference of *Drosophila melanogaster*. *Proc Natl Acad Sci*  
583 107:20051–20056.
- 584 30. Schwarzer M, Makki K, Storelli G, Machuca-Gayet I, Srutkova D, Hermanova P, Martino ME,  
585 Balmand S, Hudcovic T, Heddi A, Rieusset J, Kozakova H, Vidal H, Leulier F. 2016.  
586 *Lactobacillus plantarum* strain maintains growth of infant mice during chronic  
587 undernutrition. *Science* (80- ) 351:854 LP-857.
- 588 31. Mathiesen G, Sveen A, Brurberg MB, Fredriksen L, Axelsson L, Eijsink VG. 2009. Genome-  
589 wide analysis of signal peptide functionality in *Lactobacillus plantarum* WCFS1. *BMC*  
590 *Genomics* 10:425.
- 591 32. Xu Q, Gao W, Ding S, Kenig R, Shoham Y, Bayer EA, Lamed R. 2003. The cellulosome system  
592 of *Acetivibrio cellulolyticus* includes a novel type of adaptor protein and a cell surface  
593 anchoring protein. *J Bacteriol* 185:4548–57.
- 594 33. Artzi L, Dassa B, Borovok I, Shamshoum M, Lamed R, Bayer EA. 2014. Cellulosomics of the  
595 cellulolytic thermophile *Clostridium clariflavum*. *Biotechnol Biofuels* 7:100.
- 596 34. Zepeda V, Dassa B, Borovok I, Lamed R, Bayer EA, Cate JHD. 2013. Draft Genome Sequence  
597 of the Cellulolytic Bacterium *Clostridium papyrosolvens* C7 (ATCC 700395). *Genome*  
598 *Announc.*
- 599 35. Mingardon F, Chantal A, López-Contreras AM, Dray C, Bayer EA, Fierobe H-P. 2007.  
600 Incorporation of fungal cellulases in bacterial minicellulosomes yields viable,  
601 synergistically acting cellulolytic complexes. *Appl Environ Microbiol* 73:3822–3832.

- 602 36. Fan L-H, Zhang Z-J, Yu X-Y, Xue Y-X, Tan T-W. 2012. Self-surface assembly of cellulosomes  
603 with two miniscaffoldins on *Saccharomyces cerevisiae* for cellulosic ethanol production.  
604 Proc Natl Acad Sci 109:13260–13265.
- 605 37. Blouzard JC, Bourgeois C, De Philip P, Valette O, Bélaïch A, Tardif C, Bélaïch JP, Pagès S.  
606 2007. Enzyme diversity of the cellulolytic system produced by *Clostridium cellulolyticum*  
607 explored by two-dimensional analysis: Identification of seven genes encoding new  
608 dockerin-containing proteins. J Bacteriol 189:2300–2309.
- 609 38. Mohand-Oussaid O, Payot S, Guedon E, Gelhaye E, Youyou A, Petitdemange H. 1999. The  
610 extracellular xylan degradative system in *Clostridium cellulolyticum* cultivated on xylan :  
611 evidence for cell-free cellulosome production. J Bacteriol 181:4035–4040.
- 612 39. Haimovitz R, Barak Y, Morag E, Voronov-Goldman M, Lamed R, Bayer EA. 2008. Cohesin-  
613 dockerin microarray: Diverse specificities between two complementary families of  
614 interacting protein modules. Proteomics 8:968–979.
- 615 40. Pagès S, Belaich A, Belaich J-P, Morag E, Lamed R, Shoham Y, Bayer EA. 1997. Species-  
616 specificity of the cohesin-dockerin interaction between *Clostridium thermocellum* and  
617 *Clostridium cellulolyticum*: Prediction of specificity determinants of the dockerin domain.  
618 Proteins 29:517–527.
- 619 41. Tsai SL, DaSilva NA, Chen W. 2013. Functional display of complex cellulosomes on the yeast  
620 surface via adaptive assembly. ACS Synth Biol 2:14–21.
- 621 42. Stern J, Morais S, Lamed R, Bayer EA. 2016. Adaptor scaffoldins: An original strategy for  
622 extended designer cellulosomes, inspired from nature. MBio 7(2):e00083-16.
- 623 43. Remus DM, Bongers RS, Meijerink M, Fusetti F, Poolman B, de Vos P, Wells JM,  
624 Kleerebezem M, Bron PA. 2013. Impact of *Lactobacillus plantarum* sortase on target  
625 protein sorting, gastrointestinal persistence, and host immune response modulation. J

- 626 Bacteriol 195:502–509.
- 627 44. Bayer E a, Lamed R, Himmel ME. 2007. The potential of cellulases and cellulosomes for  
628 cellulosic waste management. *Curr Opin Biotechnol* 18:237–45.
- 629 45. Bosma EF, Forster J, Nielsen AT. 2017. *Lactobacilli* and *Pediococci* as versatile cell factories  
630 – Evaluation of strain properties and genetic tools. *Biotechnol Adv* 35:419–442.
- 631 46. Lynd L, Zyl W, McBride J, Laser M. 2005. Consolidated bioprocessing of cellulosic biomass:  
632 an update. *Curr Opin Biotechnol* 16:577–583.
- 633 47. Agapakis CM, Boyle PM, Silver P a. 2012. Natural strategies for the spatial optimization of  
634 metabolism in synthetic biology. *Nat Chem Biol* 8:527–535.
- 635 48. Krauss J, Zverlov V V., Schwarz WH. 2012. In vitro reconstitution of the complete  
636 *Clostridium thermocellum* cellulosome and synergistic activity on crystalline cellulose. *Appl*  
637 *Environ Microbiol* 78:4301–4307.
- 638 49. Xu C, Qin Y, Li Y, Ji Y, Huang J, Song H, Xu J. 2010. Factors influencing cellulosome activity  
639 in consolidated bioprocessing of cellulosic ethanol. *Bioresour Technol* 101:9560–9.
- 640 50. Kleerebezem M, Boekhorst J, van Kranenburg R, Molenaar D, Kuipers OP, Leer R, Tarchini  
641 R, Peters SA, Sandbrink HM, Fiers MW, Stiekema W, Lankhorst RM, Bron PA, Hoffer SM,  
642 Groot MN, Kerkhoven R, de Vries M, Ursing B, de Vos WM, Siezen RJ. 2003. Complete  
643 genome sequence of *Lactobacillus plantarum* WCFS1. *Proc Natl Acad Sci U S A* 2003/02/05.  
644 100:1990–1995.
- 645 51. Heiss S, Hörmann A, Tauer C, Sonnleitner M, Egger E, Grabherr R, Heini S. 2016. Evaluation  
646 of novel inducible promoter/repressor systems for recombinant protein expression in  
647 *Lactobacillus plantarum*. *Microb Cell Fact* 15:50.
- 648 52. Okano K, Yoshida S, Yamada R, Tanaka T, Ogino C, Fukuda H, Kondo A. 2009. Improved  
649 production of homo-D-lactic acid via xylose fermentation by introduction of xylose

650 assimilation genes and redirection of the phosphoketolase pathway to the pentose  
651 phosphate pathway in L-Lactate dehydrogenase gene-deficient *Lactobacillus plantarum*.  
652 Appl Env Microbiol 2009/10/13. 75:7858–7861.

653 53. Zhang J, Tang M, Viikari L. 2012. Xylans inhibit enzymatic hydrolysis of lignocellulosic  
654 materials by cellulases. Bioresour Technol 121:8–12.

655 54. Fredriksen L, Kleiveland CR, Hult LTO, Lea T, Nygaard CS, Eijsink VGH, Mathiesen G. 2012.  
656 Surface Display of N-Terminally Anchored Invasin by *Lactobacillus plantarum* Activates NF-  
657 kB in Monocytes. Appl Env Microbiol 78:5864–5871.

658 55. Peleg Y, Unger T. 2014. DNA Cloning and Assembly Methods, p. 73–87. In Valla, S, Lale, R  
659 (eds.), Methods in Molecular Biology. Springer Science+Business Media, New York.

660 56. Fredriksen L, Mathiesen G, Sioud M, Eijsink VGH. 2010. Cell wall anchoring of the 37-  
661 kilodalton oncofetal antigen by *Lactobacillus plantarum* for mucosal cancer vaccine  
662 delivery. Appl Environ Microbiol 76:7359–62.

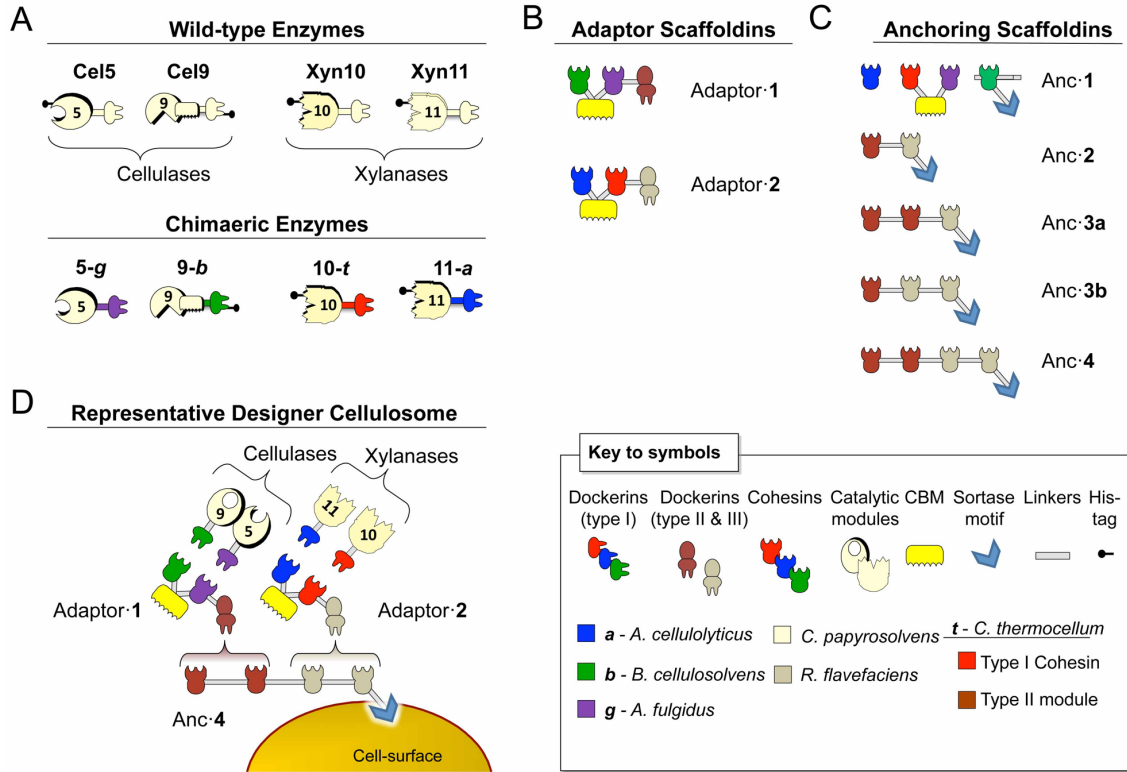
663 57. Barak Y, Handelsman T, Nakar D, Mechaly A, Lamed R, Shoham Y, Bayer EA. 2005. Matching  
664 fusion-protein systems for affinity analysis of two interacting families of proteins: The  
665 cohesin-dockerin interaction. J Mol Recognit 18:491–501.

666 58. Lapidot A, Mechaly A, Shoham Y. 1996. Overexpression and single-step purification of a  
667 thermostable xylanase from *Bacillus stearothermophilus* T-6. J Biotechnol 51:259–264.

668 59. Morag E, Lapidot A, Govorko D, Lamed R, Wilchek M, Bayer EA, Shoham Y. 1995.  
669 Expression, purification and characterization of the cellulose-binding domain of the  
670 scaffoldin subunit from the cellulosome of *Clostridium thermocellum*. Appl Environ  
671 Microbiol 61:1980–1986.

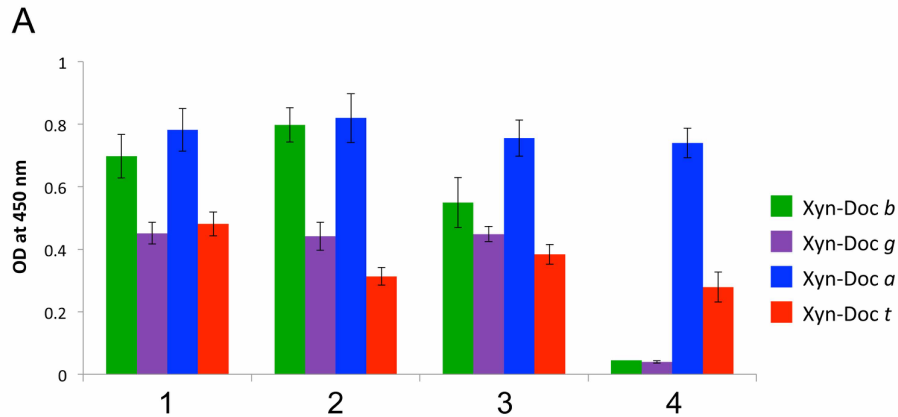
672 60. Miller GL. 1959. Use of dinitrosalicylic acid reagent for determination of reducing sugar.  
673 Anal Biochem 31:426–428.

674 61. Wegkamp A, Teusink B, Vos WM De, Smid EJ. 2010. Development of a minimal growth  
675 medium for *Lactobacillus plantarum*. Lett Appl Microbiol 50:57–64.  
676  
677



679

680 **Fig. 1.** Schematic representation of the wild-type and chimaeric proteins used in this study. The  
 681 bacterial species from which the representative modules are derived are shown color-coded in  
 682 the pictograms. (A) Wild-type and chimaeric *C. papyrosolvens* enzymes. In the shorthand notation  
 683 for the recombinant enzymes, the numbers 5, 9, 10 and 11 correspond to the GH family of the  
 684 respective catalytic modules; the origin of a given dockerin module is also indicated by lowercase  
 685 italic characters, found in the Key to symbols. (B) Modular architectures of the two different  
 686 adaptor scaffoldins designed for this work. Each adaptor scaffolding contains two divergent  
 687 cohesins for selective integration of different dockerin-containing enzymes and a type II or type  
 688 III dockerin for attachment to the appropriate cohesin-containing anchoring scaffoldin. (C)  
 689 Modular architectures of the various types of anchoring scaffoldins designed in this study. Each  
 690 contains a C-terminal sortase signal motif for covalent attachment to the cell surface. Anc-1  
 691 contains 4 divergent cohesins for selective integration of 4 different dockerin-bearing enzymes.  
 692 Anc-2 through Anc-4 are anchoring scaffoldins differing in numbers (2–4) or positions (3a, 3b) of  
 693 cohesins that integrate the two adaptor scaffoldins and their resident enzymes. (D) Example of  
 694 designer cellulosome assembly, resulting from a consortium of different strains of transformed *L.*  
 695 *plantarum*.



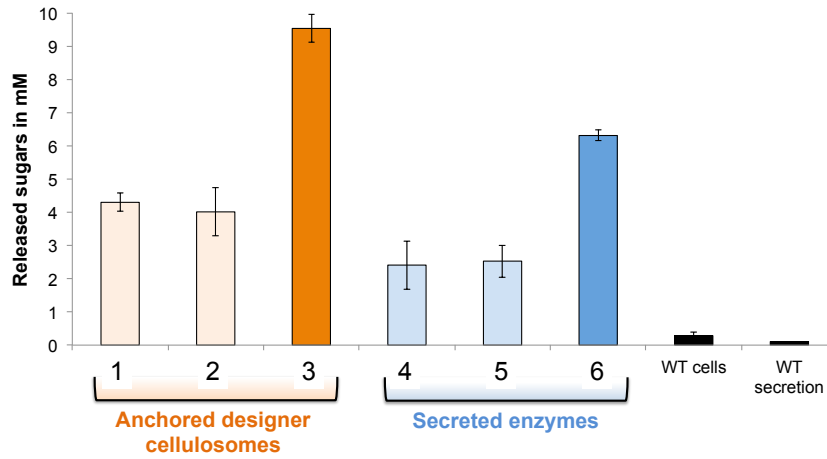
**B**

Consortium	Anchoring scaffoldin	Adaptor scaffoldin	Potential for enzyme integration	Scheme
1	Anc-2	Adaptor-1 Adaptor-2	2 Cellulases + 2 Xylanases	
2	Anc-3a	Adaptor-1 (2 units) Adaptor-2	4 Cellulases + 2 Xylanases	
3	Anc-3b	Adaptor-1 Adaptor-2 (2 units)	2 Cellulases + 4 Xylanases	
4	Anc-1	None	2 Cellulases + 2 Xylanases	

696

697 **Fig. 2.** ELISA-based binding assay demonstrating the presence of active cohesin modules on the *L.*  
 698 *plantarum* cell surface. (A) The three different consortia of individually transformed *L. plantarum*  
 699 cells (see panel B for description) and the individual *L. plantarum* strain transformed with the gene  
 700 for anchoring scaffoldin Anc-1 were examined for their capacity to interact with specific dockerin-  
 701 bearing fusion proteins. Microtiter plates were coated with 1 µg/ml of the specified dockerins  
 702 fused to the carrier protein (xylanase T6 from *G. stearothermophilus*). Washed whole bacterial  
 703 cells from transformed lactobacilli of the different consortia and the Anc-1-bearing strain were  
 704 then allowed to interact. The primary antibody used was prepared against the CBM module of the  
 705 scaffoldins. Washed bacterial cells (wild-type *L. plantarum*) served as a control. (B) Description of  
 706 the incorporated chimaeric scaffoldins for the indicated cellulosome complex. The different cell  
 707 consortia comprised the following: (1) consortium of anchoring scaffoldin Anc-2 with Adaptor-1  
 708 and Adaptor-2 (one copy each); (2) consortium of anchoring scaffoldin Anc-3a with 2 copies of  
 709 Adaptor-1 and one copy of Adaptor-2; (3) consortium of anchoring scaffoldin Anc-3b with 1 copy  
 710 of Adaptor-1 and two copies of Adaptor-2; (4) anchoring scaffoldin Anc-1.

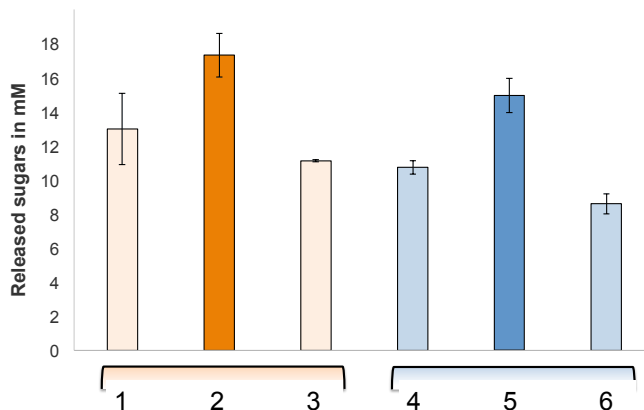
A. *L. plantarum* cell consortia (in vivo)



B. Composition of consortia and enzymes

Consortium	1	2	3	4	5	6
<b>Chimaeric enzymes – 1 unit of each enzyme = 3 nM</b>						
Xylanases 11-a, 10-t	1 unit	1 unit	2 units	1 unit	1 unit	2 units
Cellulases 9-b, 5-g	1 unit	2 units	1 unit	1 unit	2 units	1 unit
<b>Total enzymatic concentration</b>	<b>12 nM</b>	<b>18 nM</b>	<b>18 nM</b>	<b>12 nM</b>	<b>18 nM</b>	<b>18 nM</b>
<b>Chimaeric scaffoldins – 1 unit of each scaffoldin = 3 nM</b>						
Anc-2	1 unit					
Anc-3a		1 unit				
Anc-3b			1 unit			
Adaptor-1	1 unit	2 units	1 unit			
Adaptor-2	1 unit	1 unit	2 units			

C. Purified designer cellulosomes and free enzymes (in vitro)



712 **Fig. 3.** Comparative analysis of the hydrolysis of hypochlorite-pretreated wheat straw by free  
713 enzymes versus cell-associated and cell-free designer cellulosomes. (A) Soluble sugars produced  
714 in the extracellular medium by different transformed *L. plantarum* consortia versus the wild-type  
715 (WT) strain. Reactions were incubated for 96 h at 37°C. For consortia 1, 2, 3 and WT cells, washed  
716 cells were used in the enzymatic reaction, whereas for Consortia 4, 5, 6 and WT secretion cells,  
717 concentrated supernatant fluids were used. Hypochlorite-pretreated wheat straw was used at a  
718 concentration of 40 g/l, and enzymatic activities are represented by the concentration of total  
719 reducing sugars (mM). Experiments were conducted three times with triplicate samples, and  
720 standard deviations are indicated. (B) The recombinant enzymes and chimaeric scaffoldins that  
721 were introduced in the different *L. plantarum* consortia are indicated, and correspond for the  
722 respective bars in the chart. The molar ratios between the proteins, the number of units and total  
723 enzyme concentration are stipulated. (C) Soluble sugars produced by recombinant cell-free  
724 designer cellulosome assemblies and free enzyme mixtures parallel to the ones used in (A),  
725 assembled from purified proteins produced by *E. coli*. The cellulosomal components were  
726 assembled stoichiometrically, where the concentration of the anchoring scaffoldin was set at 12  
727 nM. The designer cellulosomes were allowed to assemble for 3 h at room temperature with all  
728 components of the enzymatic assay except the wheat straw substrate. The enzymatic reaction  
729 was incubated for 96 h at 37°C under shaking. Experiments were conducted three times with  
730 triplicate samples, and standard deviations are indicated.

731 **Supplementary Table Legends**

732 Table S1. Carbohydrate analysis of remaining sugars after enzymatic degradation of pre-  
 733 treated hatched wheat straw by various *L. plantarum* consortia over a 96-h incubation.

734

Enzyme combination	$\mu\text{M}$ of released sugar $\pm$ SD						
	Arabinose	Glucose	Xylose	Xylobiose	Cellobiose	Xylotriose	Cellotriose
Anchoring 1	198 $\pm$ 10	441 $\pm$ 21	159 $\pm$ 11	1794 $\pm$ 122	4 $\pm$ 0	503 $\pm$ 17	150 $\pm$ 14
Anchoring 2	102 $\pm$ 7	336 $\pm$ 27	58 $\pm$ 4	592 $\pm$ 42	42 $\pm$ 1	243 $\pm$ 5	81 $\pm$ 18
Anchoring 3	27 $\pm$ 1	672 $\pm$ 39	94 $\pm$ 8	5034 $\pm$ 145	4 $\pm$ 0	1870 $\pm$ 126	32 $\pm$ 2
Secreting 4	60 $\pm$ 9	75 $\pm$ 1	29 $\pm$ 2	1861 $\pm$ 17	7 $\pm$ 0	1134 $\pm$ 102	257 $\pm$ 13
Secreting 5	101 $\pm$ 17	109 $\pm$ 5	142 $\pm$ 30	1926 $\pm$ 184	ND	1164 $\pm$ 131	182 $\pm$ 28
Secreting 6	100 $\pm$ 8	162 $\pm$ 9	25 $\pm$ 6	2520 $\pm$ 222	ND	1773 $\pm$ 154	207 $\pm$ 11

735

736 ND, not detected

737

738

Chimearas (plasmid)	Modules	Primers	Sequence	Restriction enzyme
<b><i>C. papyrosolvens</i> chimaeric enzymes</b>				
9- <i>b</i> (pET-28a)	Catalytic subunit GH9	Forward	5'GCATTATCATGAGCGCAGGAA CATATAATTATGGAG 3'	BspHI
		Reverse	5'CCATTAGCTAGCATCAGGGTT TTCCGGTCCACC 3'	NheI
	Dockerin <i>b</i>	Forward	5'ATACAAGCTAGCCCAAAAGGC ACAGCTACAGTAT 3'	NheI
		Reverse	5'AGGCTACTCGAGCGCTTTTTG TTCTGCTGGGAAC 3'	XhoI
9- <i>b</i> pLp_2588s	Signal peptide 2588	Forward	5'CAAGGTCATATGCGCAAAAAA TGCGATGGTTATT 3'	NdeI
		Reverse	5'AATCCAGTCGACGTTGCGGGC CTGACTAACTAAG 3'	SalI
	Enzymatic subunit 9- <i>b</i>	Forward	5'AATGCAGTCGACGCAGGAACA TATAATTATGGAG 3'	SalI
		Reverse	5'GACCTAAAGCTTTTACGCTTTT TG TTCTGCTGGGAAC 3'	HindIII
5- <i>g</i> (pET-28a)	Catalytic subunit GH5	Forward	5'CCTAATCCATGGGTTATGATG CTTCACTTATTCCG 3'	NcoI
		Reverse	5'AGGCATGGTACCTTATCAGTC TGCGCTTCGAAAGC 3'	KpnI
	Dockerin <i>g</i>	Forward	5'TGGACAGGTACCAGAAGAAG CA AACAAGGGAGATG 3'	KpnI
		Reverse	5'AATATACTCGAGCTTACCCAG TAAGCCATTCTGG 3'	XhoI
5- <i>g</i> pLp_2588s	Signal peptide 2588	<i>see above (5-g)</i>		
	Enzymatic unit 5- <i>g</i>	Forward	5'AATGCAGTCGACTATGATGCT TCACTTATTCCG 3'	SalI
		Reverse	5'GAACTAAAGCTTTTACTTACC CAGTAAGCCATTCTG 3'	HindIII
11- <i>a</i> (pET-21a)	Catalytic subunit GH11	Forward	5'CTGGATGCTAGCATGCACCAT CACCATCACCACGCAACAACGA TTACTGAAAATC 3'	NheI
		Reverse	5'ATCATCGAGCTCAGGCTGAGT TCCGCCGCAAC 3'	SacI
	Dockerin <i>a</i>	Forward	5'ATTAGCGAGCTCACAGCAACT ACAACACCAACTACA 3'	SacI
		Reverse	5'CAACGTCTCGAGTTATTCCTTCT TTCTCTTCAAC 3'	XhoI

11- <i>a</i> pLp_3050s	Signal peptide 3050	<i>from previous publication</i> [1]		
	Enzymatic unit 11- <i>a</i>	Forward	5'CAGAACGTCGACGCAACAACG ATTACTGAAAATC 3'	Sall
Reverse		5'AACTTAAAGCTTTTATTCTTCT TTCTCTTCAACAGG 3'	HindIII	
10- <i>t</i> (pET-28a)	Catalytic subunit GH10	Forward	5'GAATTCCCATGGGCGCTACTC CAACAGGTACAAGG 3'	NcoI
		Reverse	5'AGACTAAAGCTTTGTAGGAGC TGTAGCGAGAGC 3'	HindIII
	Dockerin <i>t</i>	Forward	5'AATAGCAAGCTTGAAAGCAGT TCCACAGGTCTG 3'	HindIII
		Reverse	5'CCATCACTCGAGTCCGGGGAA CTCTGTAATAATG 3'	XhoI
10- <i>t</i> pLp_3050s	Signal peptide 3050	<i>from previous publication</i> [1]		
	Enzymatic unit 10- <i>t</i>	Forward	5'ATTCCAGTCGACGCTACTCCA ACAGGTACAAGG 3'	Sall
Reverse		5'AAGCGACCCGGGTTATCCGGG GAACTCTGTAATAATG 3'	SmaI	
<b>Chimaeric scaffoldins</b>				
Adaptor 1 (pET-28a)	Cohesin B, CBM3a, cohesin G*	Forward	5'GCAATCCCATGGGCGGGAAAA GTTACCAGGAAATAA3'	NcoI
		Reverse	5'GATCAAAGATCTGGCTTCTTC CTGAGAGACAATC3'	BglII
	Dockerin type II ( <i>C. thermocellum</i> )	Forward	5'TGCACCGGATCCAATAATAA ACC TGTAATAGAAG 3'	BamHI
		Reverse	5'AAAGTCCTCGAGCTGTGCGTC GTAATCACTTG 3'	XhoI
Adaptor 1 (pLp_3050s)	Cohesin B, CBM3a, cohesin G, dockerin type II ( <i>C. thermocellum</i> )	Forward	5'GCATAAGTCGACGGGAAAAGT TCACCAGGAAATAA3'	Sall
		Reverse	5'AAGATCCCCGGGTCACTGTGC GTCGTAATCACTTGATG3'	SmaI
Adaptor 2 (pET-28a)	Cohesin A, CBM3a, cohesin T*	Forward	5'CTAACGCCATGGGCTTACAGG TTGACATTGGAAGTAC3'	NcoI
		Reverse	5'GATCAGGCTAGCAACATTTAC TCCACCGTCAAAG3'	NheI
	Dockerin type III ( <i>R. flavefaciens</i> 17)	Forward	5'CAATGCGCTAGCGCTAACTAC GATCACTCCTACG3'	NheI
		Reverse	5'ACCTGGCTCGAGTTTACCGAA TCTTGCGTCTCCG3'	XhoI
Adaptor 2 (pLp_3050s)	Cohesin A, CBM3a, cohesin F, dockerin type III ( <i>R. flavefaciens</i> 17)	Forward	5'ACTGTAGTCGACTTACAGGTT GACATTGGAAGTAC3'	Sall
		Reverse	5'TCAGAACCCGGGTCATTTACC GAATCTTGCGTCTCCG3'	SmaI
ScAnc 1 (pET-28a)	Cohesin A, CBM3a, cohesins T, G, B**	Forward	5'CAATTGCCATGGGCCGGCCGC ATTTACAGGTTGAC3'	NcoI

		Reverse	5'ATTGGCCTCGAGTCAAATTGG CTTATTAGTTACAGTAATG3'	XhoI
ScAnc-1 (pLp_0373sOF A)	Cohesin A, CBM3a, Cohesins T, G, B**	Forward	5'AACGCTGTCGACCGGCCGCAT TTACAGGTTGAC3'	Sall
		Reverse	5'GATTCAACGCGTAATTGGCTT ATTAGTTACAGTAATG3'	MluI
ScAnc-2 (pET-28a)	Cohesin T <sub>2</sub> ( <i>OlpB</i> )	Forward	5'GTAAACCATGGGCGAAGCAA CTCCAAGTATTGAAATG 3'	NcoI
		Reverse	5'CAAATCGAATTCGCTGGCGTC TTTAAACGGTTCTG 3'	EcoRI
	Cohesin F <sub>3</sub> ( <i>ScaE</i> )	Forward	5'GTTACAGAATTCGGCCCCGCT GCTGGTCAGGC 3'	EcoRI
		Reverse	5'CTTAGTCTCGAGAGATGTAGT ACTCTCAACCTGG 3'	XhoI
ScAnc-2 (pLp_0373sOF A)	Cohesins T <sub>2</sub> , F <sub>3</sub>	Forward	5'CATGAAGTCGACGAAGCAACT CCAAGTATTGAAATG 3'	Sall
		Reverse	5'ATAGCAACGCGTAGATGTAGT ACTCTCAACCTGG 3'	MluI
ScAnc-3a (pET-28a)	Cohesins 2T <sub>2</sub> ( <i>OlpB</i> )	Forward	5'GTAAACCATGGGCGAAGCAA CTCCAAGTATTGAAATG 3'	NcoI
		Reverse	5'CAAATCGAATTCGGGTACAGG CTCTTCTGTCCG 3'	EcoRI
	Cohesin F <sub>3</sub> ( <i>ScaE</i> )	<i>see above (ScAnc-T<sub>2</sub>F<sub>3</sub>)</i>		
ScAnc-3a (pLp_0373sOF A)	Cohesins 2T <sub>2</sub> , F <sub>3</sub>	Forward	5'CATGAAGTCGACGAAGCAACT CCAAGTATTGAAATG 3'	Sall
		Reverse	5'ATAGCAACGCGTAGATGTAGT ACTCTCAACCTGG 3'	MluI
ScAnc-3b (pET-28a)	Cohesins T <sub>2</sub> , F <sub>3</sub>	Forward	5'GTAAACCATGGGCGAAGCAA CTCCAAGTATTGAAATG 3'	NcoI
		Reverse	5'CAAATCGCTAGCAGATGTAGT ACTCTCAACCTGG 3'	NheI
	Linker Ct-CipA, Cohesin F <sub>3</sub> ( <i>ScaE</i> )	Forward	5'AACGCTGCTAGCGGTAGTTCC GTACCGACAACACAGCCAAATG TTCCGTCAGACGGCCCCGCTGCT GGTCAGGC 3'	NheI
		Reverse	5'CTTAGTCTCGAGAGATGTAGT ACTCTCAACCTGG 3'	XhoI
ScAnc-3b (pLp_0373sOF A)	Cohesins T <sub>2</sub> , 2F <sub>3</sub>	Forward	5'CATGAAGTCGACGAAGCAACT CCAAGTATTGAAATG 3'	Sall
		Reverse	5'ATAGCAACGCGTAGATGTAGT ACTCTCAACCTGG 3'	MluI
ScAnc-4 (pET-28a)	Cohesins 2T <sub>2</sub> , F <sub>3</sub>	Forward	5'GTAAACCATGGGCGAAGCAA CTCCAAGTATTGAAATG 3'	NcoI
		Reverse	5'CAAATCGCTAGCAGATGTAGT ACTCTCAACCTGG 3'	NheI
	Linker Ct-CipA, Cohesin F <sub>3</sub> ( <i>ScaE</i> )	<i>see above (ScAnc-T<sub>2</sub>2F<sub>3</sub>)</i>		
ScAnc-4	Cohesins 2T <sub>2</sub> , 2F <sub>3</sub>	Forward	5'CATGAAGTCGACGAAGCAACT CCAAGTATTGAAATG 3'	Sall

(pLp_0373sOF A)		Reverse	5' ACCTACACGCGTGTGCTCGAG AGATGTAGTAC 3'	MluI
--------------------	--	---------	--	------

741

742

743

744 The different modules were obtained by PCR amplification from relevant genomic DNA unless  
745 otherwise specified.

746

747 \* The indicated fragments were obtained by PCR amplification from the plasmid of Scaf-CATGB  
748 from our previous report [2]

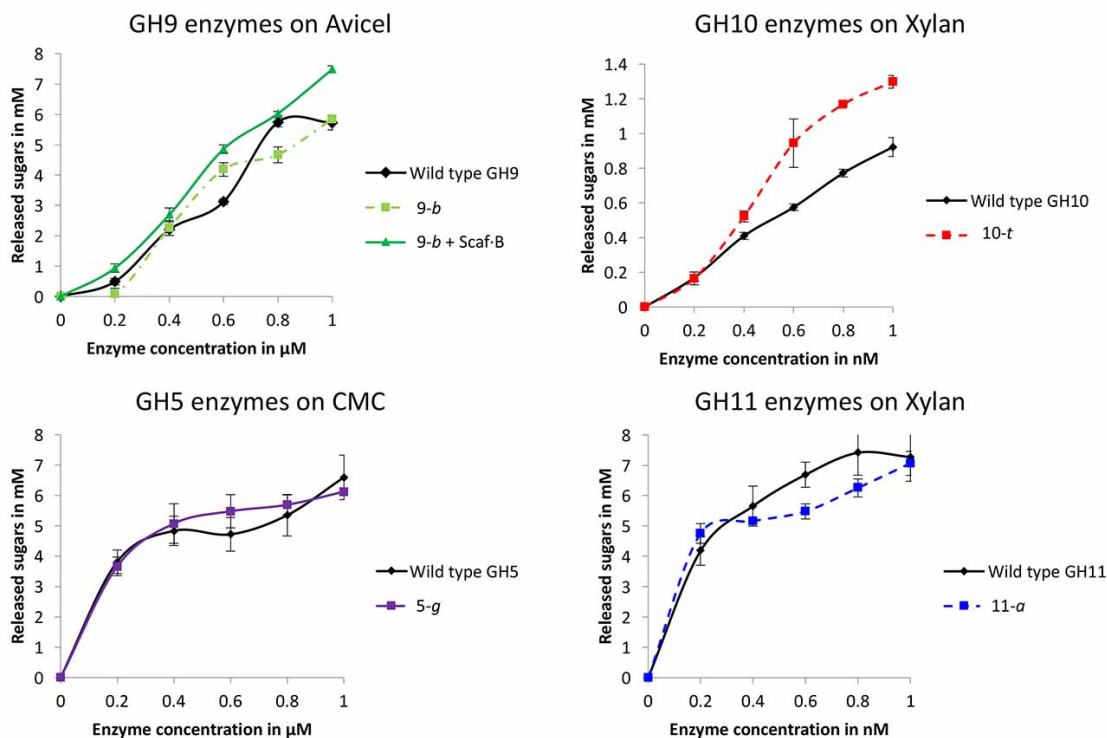
749 \*\* The indicated fragments were obtained by PCR amplification from the plasmid of  
750 Scaf-CATGB from our previous report [3]

751

752

753

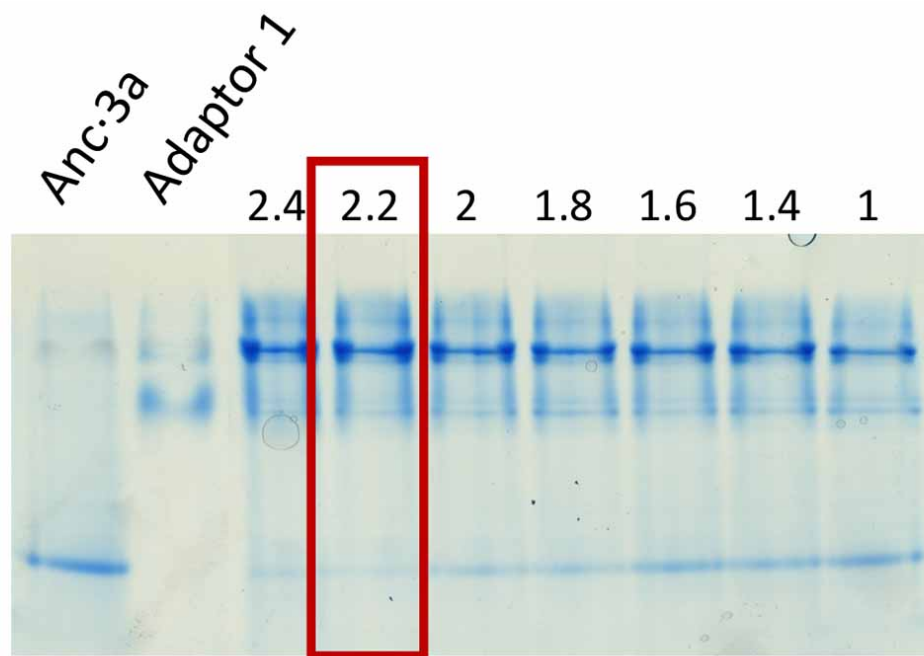
754 **Supplementary Figures**



755  
756  
757  
758  
759  
760  
761  
762  
763

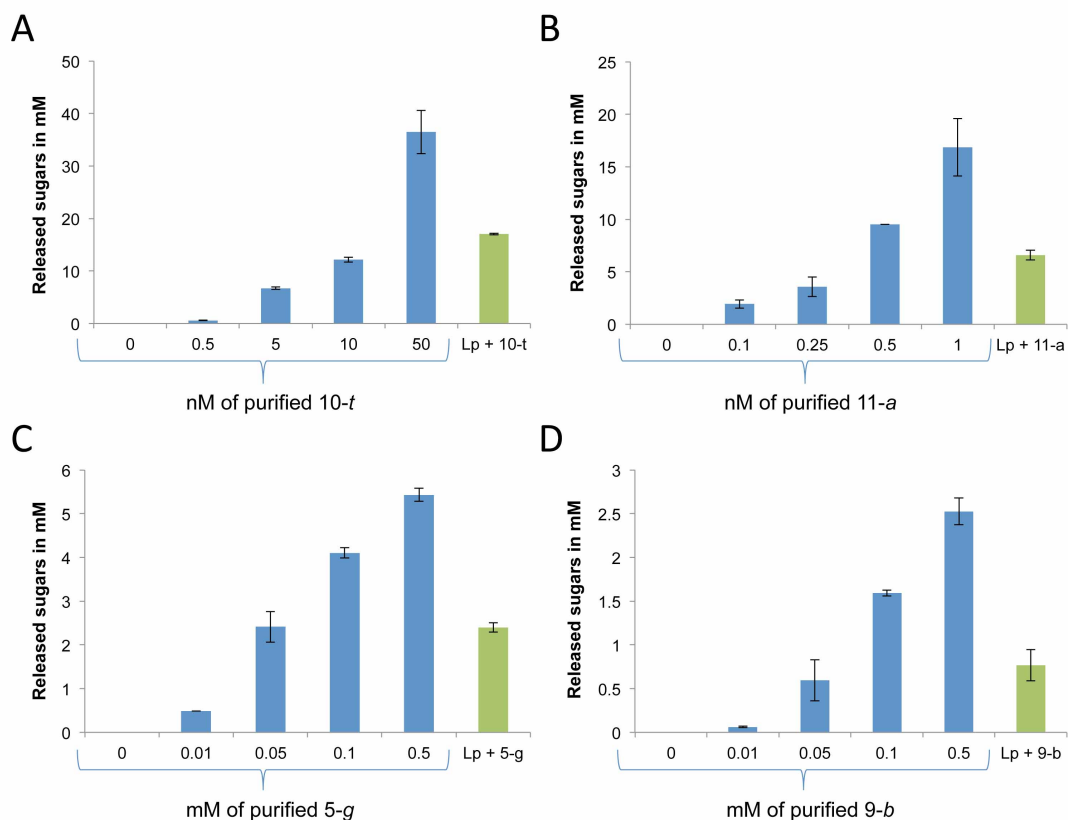
**Fig S1.** Hydrolytic activity profiles of the four recombinant *C. papyrosolvans* enzymes in comparison with the wild-type forms. The indicated enzymes were incubated 2 h at 37°C for xylan and CMC or 24 h for Avicel. Enzyme notation is given in Figure 1 of the article. Scaf-B refers to a monovalent scaffoldin, comprising the *C. thermocellum* scaffoldin-borne CBM3a and the *B. cellulosolvans* cohesin.

764



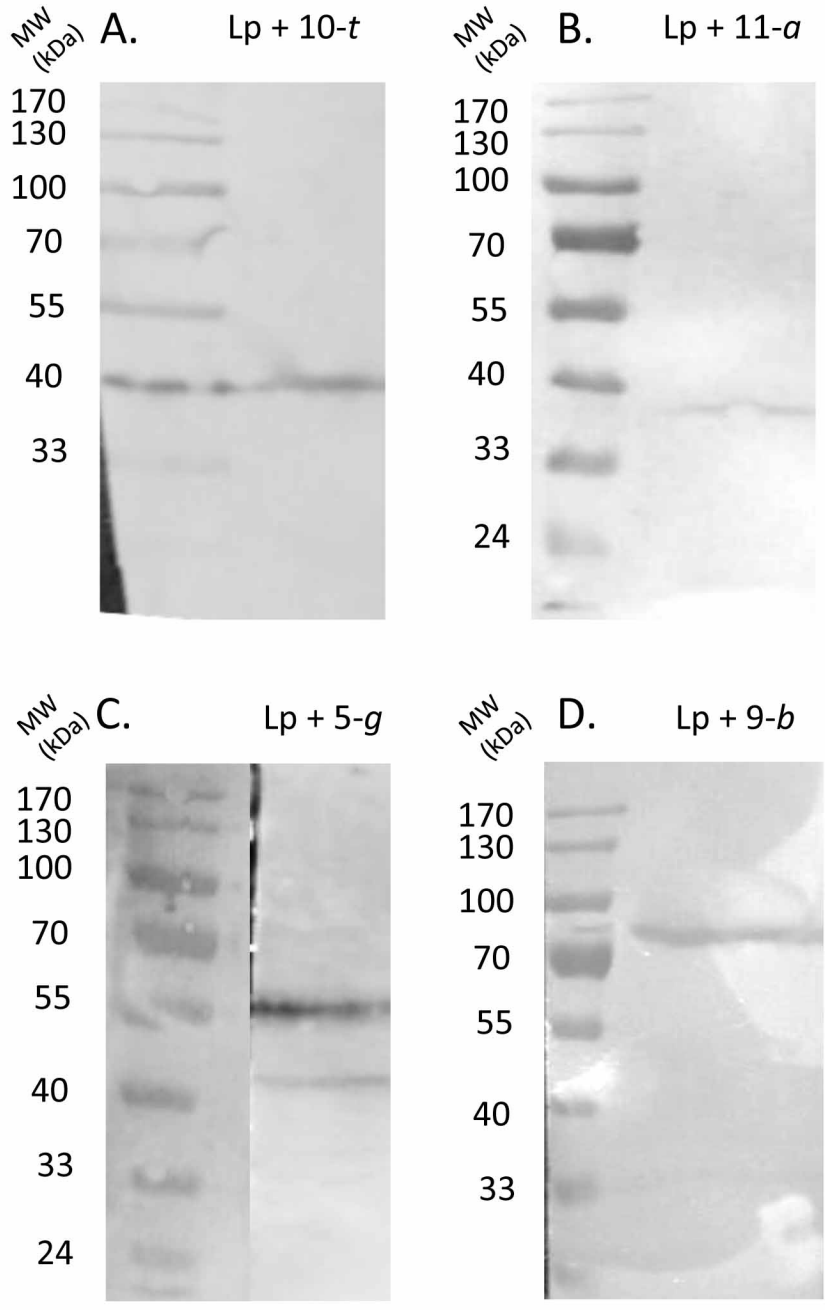
765  
766  
767  
768  
769  
770  
771

**Fig. S2.** Non-denaturing gel electrophoresis of the complex of pure recombinant Adaptor 1 with Anc-3a produced in *E. coli*. Lane 1: Anc-3a; Lane 2: Adaptor 1; Lanes 3 to 9: ratios of Adaptor 1/ Anc-3a (i.e. Lane 3, 2.4:1).



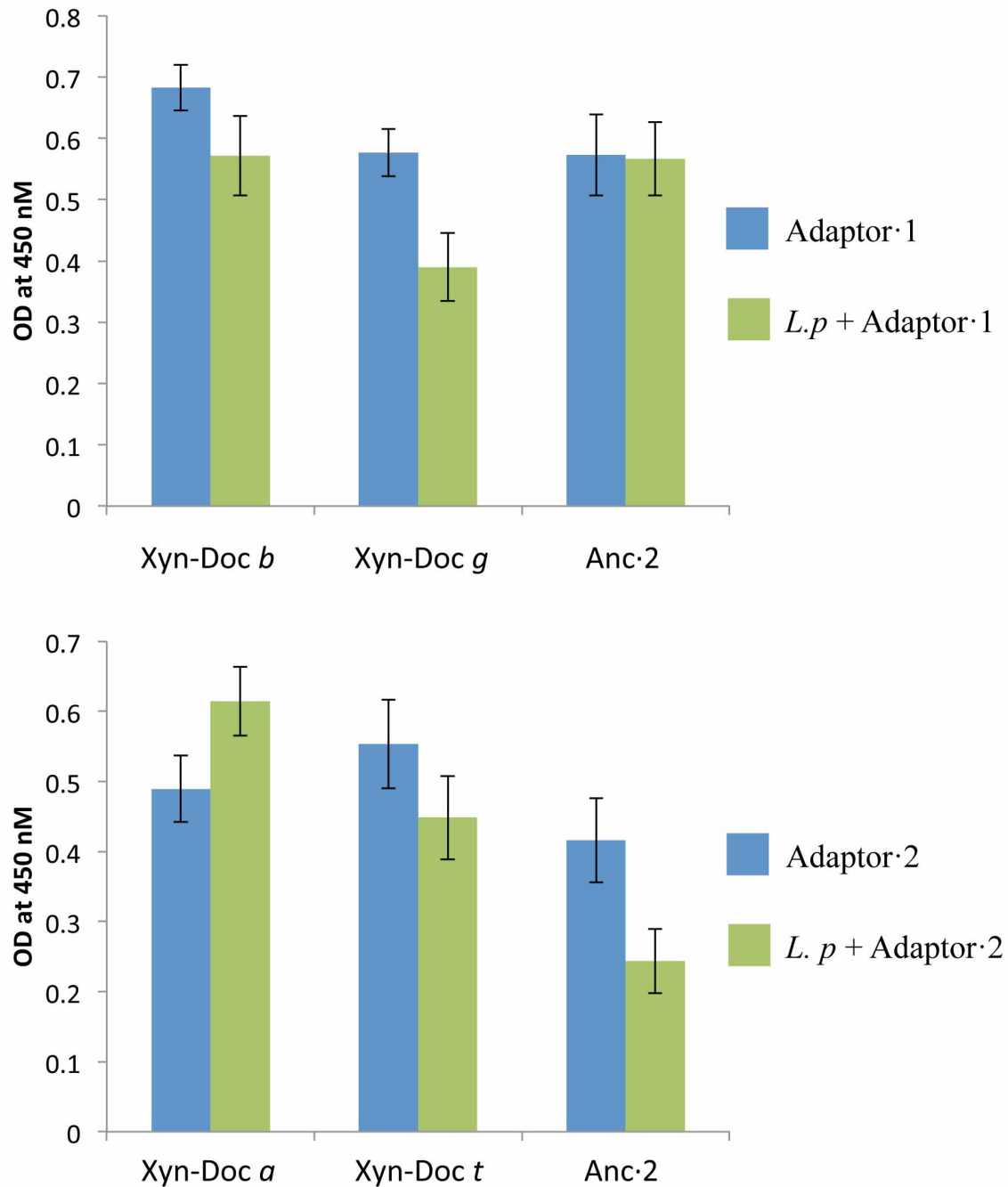
772  
773  
774  
775  
776  
777  
778  
779  
780  
781  
782  
783

**Fig. S3.** Quantification of the secreted *L. plantarum* enzymes by assessing comparative activity with known concentrations of pure recombinant proteins produced in *E. coli*. (A) and (B): enzymatic activity on xylan. Reactions were conducted with either increasing concentrations of purified *C. papyrosolvens* xylanases 10-*t* and 11-*a*, respectively, or with 30  $\mu$ l of concentrated culture supernatant fluids, following a 2-h reaction period at 37°C. (C) and (D): enzymatic activity on carboxymethyl cellulose (CMC). Reactions were conducted with either increasing concentrations of purified *C. papyrosolvens* cellulases 5-*g* and 9-*b*, respectively, or with 30  $\mu$ l of concentrated culture supernatant fluids following a 2-h reaction period at 37°C.



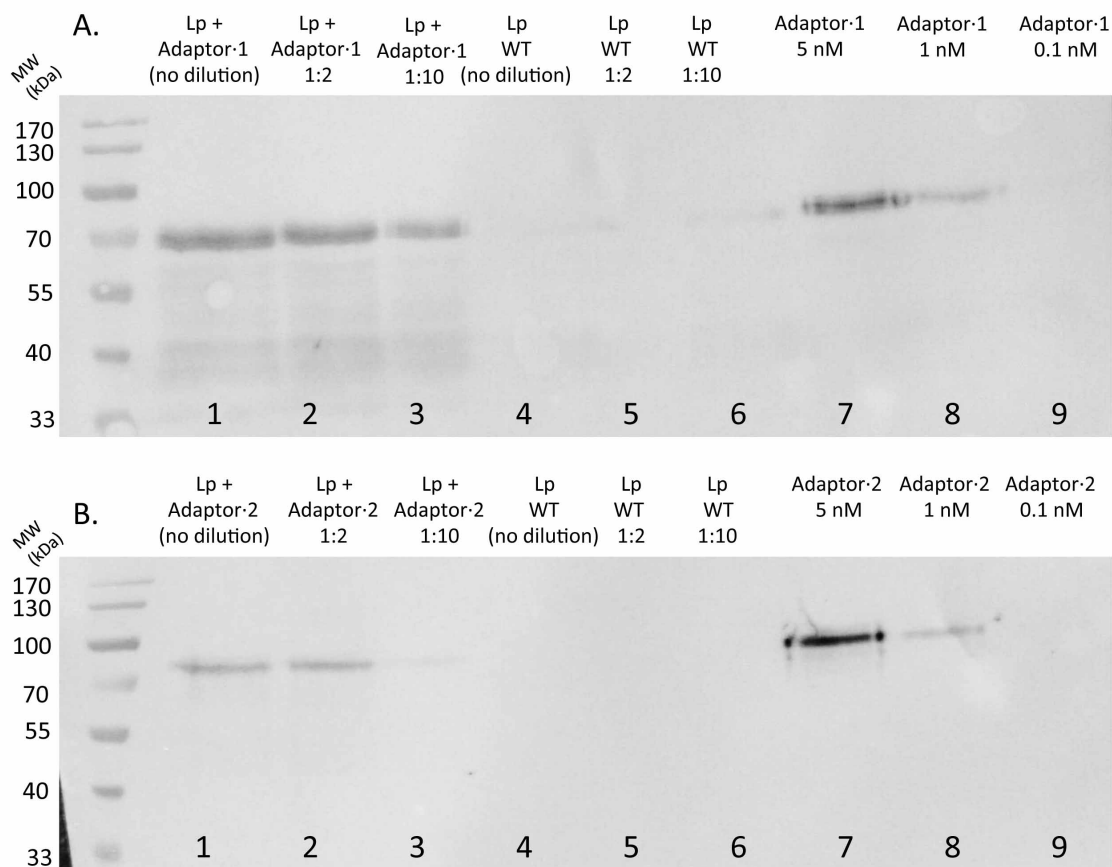
784  
785  
786  
787

**Fig. S4.** Far-Western blot analysis (A, B, C and D) and Western blot analysis (E and F) of concentrated culture supernatant fluids from transformed lactobacilli versus respective pure recombinant proteins produced in *E. coli*. (A) Secreted 10-*t* (calculated mass 44.5 kDa), (B) secreted 11-*a* (calculated mass 33 kDa), (C) secreted 5-*g* (calculated mass 51.3 kDa), (D) secreted 9-*b* (calculated mass 77.6 kDa). (E) and (F): The lanes in the two panels (E) Adaptor-1 (calculated mass 79.3 kDa) and (F) Adaptor-2 (calculated mass 72.8 kDa) are as follows: Lanes 1-3: secreted Adaptor by *L. plantarum*; Lane 4-6: secreted fraction of wild-type *L. plantarum*; Lane 7-9: pure Adaptor produced by *E. coli*.



796  
797  
798  
799  
800  
801  
802  
803  
804  
805

**Fig. S5.** ELISA-based binding assay of pure recombinant proteins produced in *E. coli* versus concentrated secreted proteins from transformed *L. plantarum*. Microtiter plates were coated with 1  $\mu$ g/ml the purified proteins as specified in the X axis and subjected to interaction with either 100 ng/ml of pure adaptor scaffoldin (blue bars) or *L. plantarum* secreted adaptor scaffoldin (green bars). The primary antibody used here was elicited against the CBM of the scaffoldins (i.e., CBM3a of the *C. thermocellum* CipA scaffoldin). Concentrated secreted proteins from *L. plantarum* wild-type strain were used as a blank.



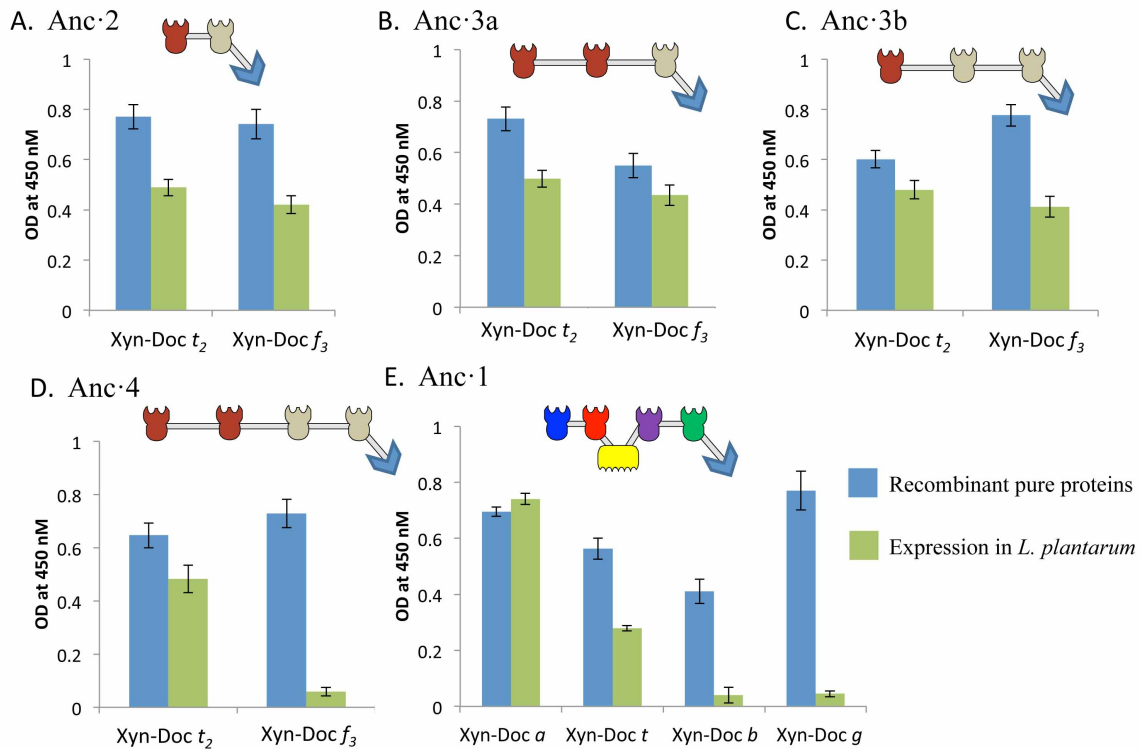
807

808

809

810 **Fig. S6.** ELISA binding assay of pure recombinant proteins produced in *E. coli* versus anchored  
 811 proteins produced by *L. plantarum*. Microtiter plates were coated with 1  $\mu\text{g}/\text{ml}$  of pure proteins  
 812 produced in *E. coli* as specified in the x axis and subjected to interaction with either 100 ng/ml of  
 813 pure chimaeric scaffoldin produced in *E. coli* (blue bars) or *L. plantarum* cells displaying the  
 814 anchored scaffoldin (green bars). The primary antibody used for panels A, B, C and D was elicited  
 815 against the type II cohesin from *C. thermocellum*, present on Anc-T<sub>2</sub>F<sub>3</sub> (Anc 2), Anc-2T<sub>2</sub>F<sub>3</sub> (Anc 3a),  
 816 Anc-T<sub>2</sub>2F<sub>3</sub> (Anc 3b) and Anc-2T<sub>2</sub>2F<sub>3</sub> (Anc 4), where T<sub>2</sub> represents the type II *C. thermocellum*  
 817 cohesin and F<sub>3</sub> represents the type III *R. flavefaciens* cohesin; for panel E, the primary antibody  
 818 was elicited against the CBM of Anc-1. Washed bacterial cells (wild-type strain) served as a control.  
 819

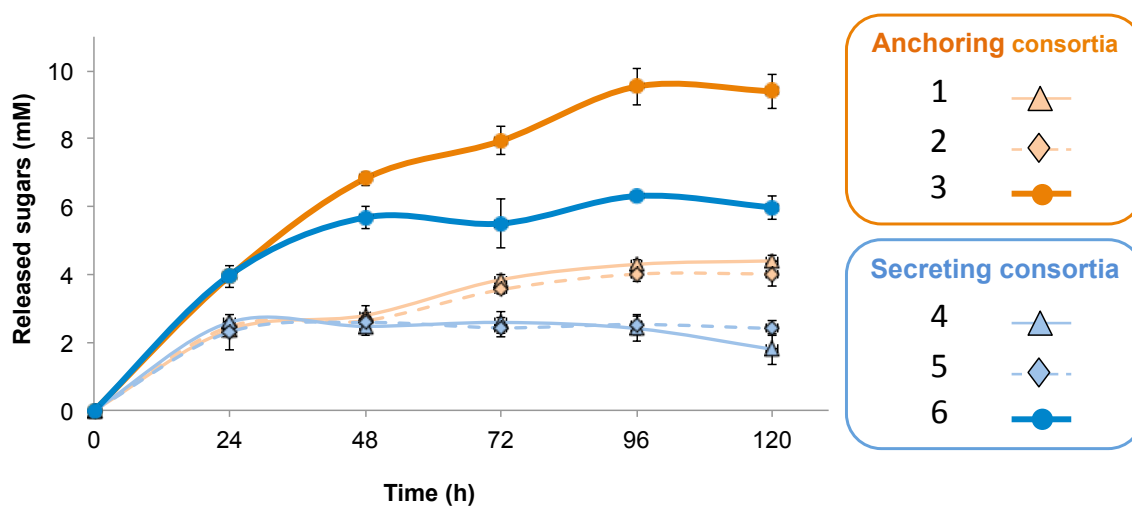
819



820  
821  
822  
823  
824  
825  
826  
827

**Fig.S7.** Kinetics studies of hypochlorite-treated wheat straw hydrolysis up to 120-h incubation at 37°C by the different types of consortia. The composition of the consortia is as specified in Figure 3 panel B. Enzymatic activity is defined as total reducing sugars released ( $\mu\text{M}$ ). Error bars show standard deviations.

828



829

830

831 **Fig. S8.** Bacterial growth on incremental concentrations of sugars with chemically defined medium

832 CDM supplemented with (A) cellobiose, and (B) glucose. Xylose and xylobiose as sole carbon

833 sources could not sustain growth.

834